

1 We thank both reviewers for their thoughtful and constructive comments. Revising the paper  
2 to address their concerns has significantly improved the manuscript. We have addressed the  
3 concerns expressed in the reviews as completely as possible in the point-by-point responses  
4 and in the revised paper. The reviewers' comments are in black font and our responses are  
5 below each comment in blue font.

6 **Reviewer #1**

7 **I General Comments**

8

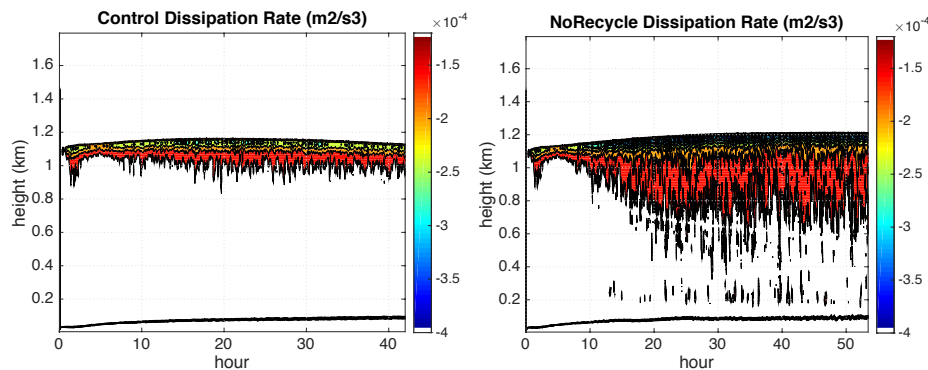
9 This study investigates the persistence and liquid-ice phase partitioning of mixed-phase  
10 stratocumulus clouds typical of the Arctic. The authors suggest that subcloud ice crystal  
11 sublimation produces ice nuclei that recycle back into the cloud layer to reactivate ice  
12 particles. The recycling of ice nuclei act to maintain the ice water content over a longer time-  
13 scale than without recycling, and with the combination of cloud-top radiative cooling, both  
14 liquid and ice contents can be steadily maintained. The authors also imply a diurnal impact  
15 on the maintenance of mixed-phase stratocumulus in that both liquid and ice productions are  
16 weakened in the presence of shortwave radiation, which in turn reduces ice precipitation  
17 fluxes out of the layer, and hence further prolonging the lifetime of the system.

18 Previous studies on the maintenance of mixed-phase stratocumuli involve the discussion of  
19 the rapid glaciation and dissipation of these clouds due to efficient ice depositional growth  
20 via the evaporation of the liquid content, usually at higher ice concentrations. Because ice  
21 nuclei recycling effectively maintains a consistent ice concentration, it would be curious to  
22 see what role recycling would play in liquid/cloud dissipation rates.

23

24 The dissipation rates are proportional to the TKE in each run. Here are figures of the  
25 dissipation rates for Control and NoRecycle:

26



27

28 Maximum TKE in NoRecycle is ~28% larger than Control because of the larger LWP which  
29 is consistent with the ~32% increase in the maximum dissipation rate.

30

31 Furthermore, figures 7a and 10a indicate that, over time, the liquid water content achieves  
32 higher values when the diurnal cycle is consistent, in contrast to the ice water content, which  
33 drops to lower values. This result is not discussed, but one would imagine that the diurnal  
34 cycle would also help to maintain a mixed-phase cloud that would otherwise dissipate.

35  
36  
37  
38  
39  
40  
41  
42  
43  
44  
45  
46  
47  
48  
49  
50  
51  
52  
53  
54  
55  
56  
57  
58  
59  
60  
61  
62  
63  
64  
65  
66  
67  
68  
69  
70  
71  
72  
73  
74  
75  
76  
77  
78  
79  
80

On page 11742 line 9 we have added, "...and promotes the persistence of a mixed-phase cloud system."

The work presented is very interesting and compelling. The recycling technique appears to compare well with previous work that employ relaxation ice concentration methods for simpler studies, and so perhaps the recycling effect could be considered a motivation for simulations with assumed constant ice concentrations. The manuscript is well written, concise, and organized thoughtfully. The manuscript content and figures, however, are very compact and complex, so I would urge the authors to consider simplifying and/or shortening sentences throughout for ease of reading. I would also encourage the authors to simplify figures so that they are easier to interpret.

Thank you, we have gone through the manuscript to identify sentences that can be simplified and shortened.

With the advice given above and the suggestions listed below, my recommendation for this manuscript is *accept for publication with major revisions*.

## 2 Specific Comments

1. Page 11729, Lines 4-7, "However, unlike subtropical...at cloud top": Which process are considered to dissipate subtropical mixed-phase clouds that do not occur in the Arctic? One would imagine that subtropical clouds could also be supplied with moist air at cloud top. Are AMPS unique from all other mixed-phase stratocumuli in other regions (e.g., midlatitudes)? If so, is there a specific quality (e.g., temperature, solar zenith) in AMPS to contribute to these differences?

This sentence has been changed to read, "However, unlike subtropical cloud-topped boundary layers where decoupling enhances cloud breakup by cutting the cloud system off from the surface source of moisture, decoupled AMPS can persist for extended periods of time due to weak precipitation fluxes out of the mixed layer and relatively moist air entrained into the cloud layer at cloud top."

2. Page 11730, Line 22, "We posit that recycling...": The term "recycling" has been used many times thus far, but has never been defined or conceptually explained.

A clarifying sentence has been added on page 11730 at line 12, "This feedback loop is referred to hereon as "recycling".

3. Page 11730, Line 27, "...while AMPS...": Perhaps change to "...while persistent AMPS". AMPS are not necessarily always persistent, so please be sure to differentiate throughout.

Sentence changed as suggested.

- 81 4. Page 11731, Line 2: Please indicate whether recycling is turned off or on for the Control  
82 simulation as it is never indicated.  
83  
84 Lines 3-4 have been changed to, "...with recycling turned on and shortwave radiation  
85 turned off (to compare with previous simulations of this case that use different IN  
86 formulations and shortwave radiation turned off)..."  
87
- 88 5. Page 11735, Line 2: Are the IN that are produced via sublimation always recycled back  
89 into the layer? Is it possible that some IN become "inactive" after sublimation?  
90  
91 Yes, recycling just means IN become available for activation but the extent to which  
92 they become active depends on large-scale circulation, mixing by turbulent eddies, and  
93 the in-situ temperature and water vapor. The sentence has been left unchanged.  
94
- 95 6. Page 11735, Lines 8-13: Interpretation of figure 2 is unclear. Do you only consider  
96 activation at these threshold temperatures, or would a concentration of 1.3-1.5/L  
97 nucleate at -20 versus 0.75/L at 15°C? What is unique about these temperatures that  
98 make them "threshold"?  
99  
100 "used to initialize IN number concentration in each bin" has been added to the Figure 2  
101 caption. After initialization prognostic equations for each bin that include advection,  
102 turbulent mixing, and sources and sinks are used to calculate the evolution of IN in each  
103 bin. The threshold temperatures are a representation of the dependence of nucleation on  
104 surface characteristics and size. The nucleation scheme used in this study approximates  
105 this relationship with the number of IN available as a function of a threshold temperature  
106 (given the discrete bins used in this study) based on the empirical study of DeMott et al.  
107 (2010). Threshold temperatures are only needed because we are discretizing the  
108 continuous relationship shown in Figure (2).  
109
- 110 7. Page 11735, Line 22: What is the importance of the "modification of activation  
111 thresholds" and why is this consideration unnecessary for this work?  
112  
113 The sensitivity of ice nucleation to the preactivation of IN is an interesting topic but  
114 outside the scope of this study since it is so poorly defined by measurements at this time.  
115 This will be included in future studies if laboratory studies can quantify the impact of  
116 preactivation on ice nucleation.  
117
- 118 8. Page 11736, Lines 13-14: "Crystal size...Fig. 5": Why would the maximum ice size (5  
119 mm) be larger than the maximum snow size (0.7 mm) in Figure 5? What are the shape or  
120 aspect ratios and densities considered for snow and ice? What are the physical processes  
121 considered for snow and ice?  
  
122 "ICE" and "SNOW" need to be reversed in the legend in Figure 5. This has been  
123 corrected. In our model setup, the particles are assumed to be spherical and  $d$  is set equal  
124 to 3. The bulk density of ice is assumed to be  $0.5 \text{ g cm}^{-3}$  and the bulk density of snow is

125 assumed to be  $0.1 \text{ g cm}^{-3}$ . Beside the nucleation parameterization described in the paper,  
126 ice and snow mass can change due to riming, condensation/deposition, and  
127 autoconversion.

128 9. Page 11736, Line 24: To interpret figure 6, it would help to mention that IN are “lost” to  
129 activation of ice crystals.

130 The sentence has been changed to read, “IN are produced by sublimation of ice crystals  
131 below the cloud layer, advected to the cloud layer by turbulence, and removed from the  
132 population when activated as ice crystals”

133 10. Page 11737, Lines 15-23, “Over the...subcloud layer”: If the cloud was coupled, could  
134 you expect different results since rather than the turbulent eddies sweeping the IN back  
135 into the cloud, the IN could sediment to lower levels and not be recycled.

136 Yes, if the cloud becomes coupled to the surface layer then eddies can mix IN in layers  
137 from the surface to the cloud base into the cloud layer and the IN reservoir at the base of  
138 the mixed layer is quickly activated. This causes more IN to be lost from the system  
139 through increased precipitation.

140 11. Page 11737, Lines 23-25, “The continuous...mixed-layer base.” This statement is  
141 unclear. Is this statement suggesting a “residence time” effect in that IN are advected  
142 into the cloud layer out of the subcloud layer more quickly than new IN produced via  
143 crystal sublimation?

144 Yes, this is correct. There is a continual depletion of IN from below the cloud layer  
145 while the ice number concentration decreases more slowly. This is seen clearly in  
146 Figures 8b and 10e where sublimation is less than the IN flux at cloud base. The  
147 sentence has been left unchanged.

148  
149  
150 12. Figure 7b: Perhaps this is already explained, but why does the temperature warm more  
151 for recycling? Perhaps recycling induces activation which increase the release of latent  
152 heat? This should be discussed.

153 The temperature is colder for the NoRecycling case because there is more liquid in the  
154 cloud and therefore stronger cloud top cooling, which is mixed downward by cloud-  
155 driven turbulent mixing. Differences in latent heat release are not as significant as  
156 differences in radiative cooling at cloud top (not shown). A sentence has been added on  
157 page 11738 line 13, “Increased cloud liquid water when recycling is turned off results in  
158 increased radiative cooling at cloud top, which causes the cloud-driven mixed layer to  
159 cool more rapidly (Figure 7b).”

160  
161  
162 13. Figure 7d: Please explain the units m L (meters/liter?).

163 In Figure 7 caption “(meters/liter)” added.  
164  
165

166  
167 14. Figure 10c (number in column): The feedback loop in figure 9 is not apparent in figure  
168 10c as one would expect oscillations in  $N_{NI}$  to correspond with those in  $N_{IN}$ .  
169  
170 This would only be the case if precipitation, turbulent mixing and entrainment are  
171 negligible, which is not the case for this simulation. The schematic has been left  
172 unchanged.

### 173 3 Technical Corrections

174 15. Page 11729, Line 10: “radiatively-important” should be “radiatively important”.

175 Changed as suggested.

176 16. Page 11729, Line 26: Please replace the semi-colon (;) with either a colon (:) or a  
177 comma (,).

178 Changed as suggested.

179 17. Page 11729, Line 28: Please remove the first “or”.

180 Changed as suggested.

181 18. Page 11730, Line 11: Both “large-eddy” and “large eddy” have been used.

182 “large-eddy” has been replaced with “large eddy”.

183 19. Page 11730, Line 13: While it may be obvious to most readers, please consider  
184 expanding D.O.E.

185 Changed as suggested.

186 20. Page 11733, Line 7: “horizontal resolution” should be “horizontal resolutions”

187 Changed as suggested.

188 21. Page 11733, Line 23: Please replace “amplitude” with “amplitudes”.

189 Changed as suggested.

190 22. Page 11733, Line 28: Please replace “...where the slope of liquid-ice static energy  
191 exceeds...” with “...where the slopes of liquid-ice static energy exceed...”

192 Changed as suggested.

193 23. Page 11734, Line 28: Water vapor mixing ratio has already been defined.

194           Second definition removed.

195       24. Page 11739, Line 13: “Figure” should be “Figures”.

196           Changed as suggested.

197       25. Page 11741, Line 8: “control” to indicate the control case is sometimes capitalized  
198           and other times not.

199           “Control” is used uniformly throughout the paper.

200       26. Page 11742, Please consider absorbing the first paragraph into the second as the first  
201           paragraph contains only one sentence.

202           Changed as suggested.

203       27. Figure 1: There is an overlap in the x-axes of the two plots. Also, the caption  
204           indicates “grey shading” that does not appear in the figure.

205           The figure has been corrected.

206       28. Figure 3: Please add a legend.

207           A legend has been added.

208       29. Figure 4: This caption is very difficult to follow. Perhaps consider removing the first  
209           three sentences as that information is contained in the image. Also, please add the  
210           “control” lines to Figs. 4B and D and legends to B-D.

211           Thank you for your comment but we would like to keep the first three lines in the  
212           caption to identify the fields plotted in each figure. The wording of the caption has  
213           been simplified to clearly specify the fields plotted in each panel. Control LWP and  
214           IWP have been added to 4B and 4D. Legends are now in all four panels.

215       30. Figure 6 and throughout: Please consider relabeling the number of ice crystals to  
216           something like  $N_i$  as  $N_{IN}$  and  $N_{NI}$  are very easily confused.

217           “ $N_{NI}$ ” and “ $T_{NI}$ ” have been changed to “ $N_{ICE}$ ” and “ $T_{ICE}$ ” to clearly distinguish from  
218           “ $N_{IN}$ ” and “ $T_{IN}$ ”.

219       31. Figures 7a and b: Are IWP and temperature calculated for just within the cloud,  
220           within the mixed layer, or for the entire domain.

221           IWP and minimum temperature are calculated for the entire column. The caption has  
222           been changed to read, “Minimum horizontally-averaged temperature in the column, in  
223           units of °C.”

224 32. Figures 7, 8, and 10 are missing plot labels as referenced in the captions (e.g., a, b, c,  
225 d) and x-axes.

226 [Labels and axes added.](#)

227 33. Figure 10: “CB”, “CL”, and “ML” should be defined in the caption. Also, what do the  
228 grey shaded columns indicate?

229 [All abbreviations and shading are now defined in the figure caption.](#)

230

231 **Reviewer #2**

232 This manuscript investigates the role of IN recycling from the sub-cloud layer on the  
233 persistence of mixed-phase conditions in springtime Arctic stratiform clouds. The study is  
234 based on long Large Eddy Simulations of a single mixed-phase stratiform cloud case using  
235 prognostic IN concentrations. Several aspects of the problem that deserved more attention  
236 from the modeling community are addressed in this work. For example, the role of IN  
237 recycling has been isolated here from other potential sources of ice forming particles. In  
238 addition, the persistence of mixed-phase clouds has been investigated for rather long periods  
239 of time, up to 3 full diurnal cycles (including short-wave solar radiation), when most other  
240 LES studies rarely exceed 12-24h. The results and methods presented are thus particularly  
241 relevant for the field, and give new insights into the processes maintaining long-lived Arctic  
242 mixed-phase stratiform clouds.

243 I would therefore strongly recommend the publication of this article in ACP. Several issues  
244 need however to be addressed in order to improve the overall clarity of the manuscript.

245 **Major comments:**

246 First of all, a more detailed description of the prognostic IN method is required to fully  
247 understand the modeling approach and help interpret some of the results. If I understood  
248 correctly, there exists two requirements for IN particles within a given bin to activate: 1) the  
249 in-situ temperature must exceed the threshold temperature assigned to the bin, and 2) local  
250 conditions must be at or exceed water saturation. But how is the nucleation tendency  
251 calculated (activation term in equation 1)? I guess that the number of particles within bin  $k$  is  
252 initially given by the number of IN calculated by equation 2 at the threshold temperature  $k + l$   
253 minus that calculated at temperature  $k$ . But are all the particles (or 50% of them) within bin  
254  $k$  activated instantaneously as soon as the threshold temperature  $k$  is exceeded (at or above  
255 water saturation)? In other words, is ice nucleation considered to be an instantaneous process  
256 or is it allowed to vary smoothly in time? This may be of importance as IN recycling  
257 involves interactions between sublimation, droplet activation and freezing, with droplet  
258 activation often considered to occur instantaneously, and ice nucleation being a much slower,  
259 and thus limiting, mechanism.

260 Yes, this is correct. IN number concentrations are initially specified using equation 2, such  
261 that the initial IN in bin  $k$  is equal to the number of IN calculated by equation 2 at the  
262 threshold temperature  $k + l$  minus that calculated at temperature  $k$ . After the initial time 50%  
263 of the IN available in a bin nucleates if the in-situ temperature is above the threshold  
264 temperature and the local conditions exceed water saturation. This approach is motivated by  
265 the study of Ervens and Feingold (2013; doi:10.1002/grl.50580), where it was shown that, for  
266 Classical Nucleation Theory, nucleation rates are far more sensitive to temperature (T) than  
267 to time. If we consider the same nucleation rate, an uncertainty of  $\Delta T = +/- 0.2$  K translates  
268 to the same uncertainty as differences in time of about two orders of magnitude.

269  
270 Regarding observations of time dependent nucleation as in Westbrook and Illingworth:  
271 Ervens and Feingold (2013) note that "Based on our analysis, we estimate that differences of



272 five orders of magnitude in  $t$  (10s vs. 1day) are equivalent to a change of  $\Delta T \sim 2K$  (at  $T$   
273  $\sim 258K$ , i.e., the approximate  $T$  of the observed clouds)." This happens to be the same  $T$  as  
274 our Arctic case. So observations that suggest a time dependence might actually be masking  
275 small(ish)  $T$  fluctuations that are hard to measure at high spatial temporal resolution.  
276 However, temporal aspects of nucleation may play an interesting secondary role and is  
277 currently an active area of research. These temporal aspects need to be investigated in a  
278 Lagrangian model since in an Eulerian model temporal information is not available.  
279 Therefore, within the model framework of an Eulerian bin model we can represent IN  
280 distributions as a function of temperature but not time.

281 Also, is the  $F$  factor used in equation 2 applied at each time-step, i.e. is the number of  
282 activated IN after each time-step equal to 50% of the unactivated particles within the bin at  
283 the beginning of the time-step?

284 Yes, this is correct. As discussed above, the factor  $F$  is applied at every time step such that  
285 50% of the unactivated IN nucleate if the in-situ environment is saturated with respect to  
286 water and the in-situ temperature is above the threshold temperature for that bin.

287 Finally, can you please comment on the relevance of omitting the dependence of IN  
288 nucleation on water and ice saturation? In particular, assuming that IN particles are available  
289 for nucleation as soon as water saturation is reached suggests that the particles acting as IN,  
290 whatever they are, activate as cloud droplets at water saturation, regardless of their size and  
291 composition. Should we expect different conclusions on the role of IN recycling if activation  
292 and freezing were assumed to be size and composition dependent (and thus more sensitive to  
293 water saturation)?

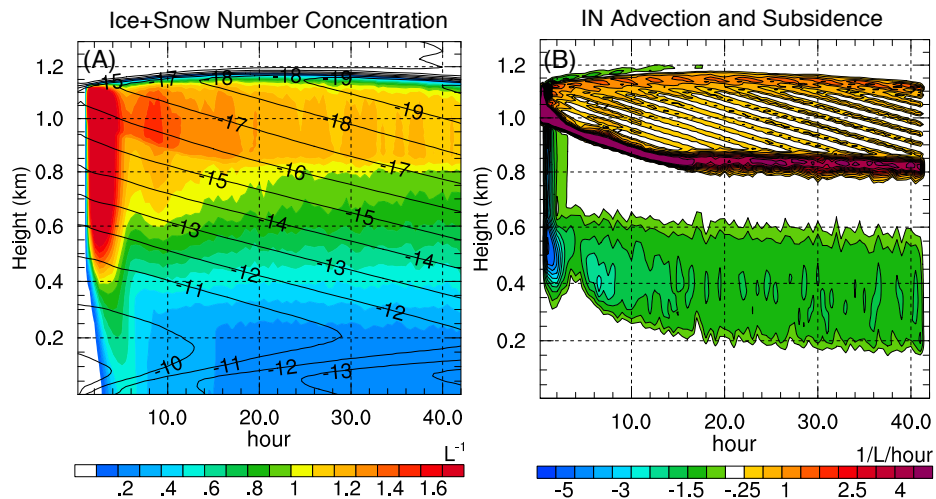
294 Yes, we are only including ice nucleation where drops are a necessary precondition. We are  
295 actually including the dependence of IN nucleation on water and ice saturation by using an  
296 empirical relationship between IN and temperature to specify the initial IN number  
297 concentrations in each bin. The number of IN available for nucleation in each bin is an  
298 implicit function of temperature, composition, and size. This is the simplest parameterization  
299 for IN that doesn't include aspects of nucleation that the model cannot resolve.

300 The results section is very concise, with very clear figures, and gives the essential  
301 information needed to understand the outcome of the study. The analysis of IN and NI fluxes  
302 through cloud base provides interesting insights on the mechanisms involved in the  
303 maintenance of IN concentrations sufficient to sustain mixed-phase cloud conditions.  
304 However, several points deserve clarifications. First of all, Figure 6 shows that ice production  
305 and IN activation are larger around cloud base. This result seems to contradict former  
306 modeling studies showing that ice formation primarily occurs at cloud top, where the  
307 temperature is lower. A short discussion of the vertical distribution of IN activation, which  
308 peaks at cloud base, may provide interesting information.

309 A figure has been added of the time evolution of the horizontally-averaged ice+snow number  
310 concentration and IN advection+subsidence (shown below in Figure S1). This figure shows  
311 that the majority of IN activates at cloud base, which is a bit warmer than cloud top but is

312 sufficiently cold to activate many of the IN. However, IN from bins with colder threshold  
 313 temperatures are advected higher into the cloud where they activate at their threshold  
 314 temperature. A secondary maximum is seen at cloud top where the coldest temperatures are  
 315 found. Also, it is seen that IN are advected into the cloud layer at cloud top for the first 15-18  
 316 hours, but this source of IN decreases as IN in the upper entrainment zone are depleted.

317 Regarding how this fits with other model studies, the location of particle nucleation is based on  
 318 on how IN processes are specified in each model. If nucleation is simply diagnosed based on  
 319 temperature, then it will occur more towards cloud top. The use of a prognostic equation to  
 320 describe IN evolution in this study causes there to be a source of IN below the mixed-phase  
 321 cloud layer that can nucleate ice given the right conditions near cloud base. Observationalist,  
 322 such as Alexei Korolev, have suggested from measurements that all sizes of frozen  
 323 hydrometeors are observed near cloud top (suggesting turbulent mixing of hydrometeors  
 324 within the cloud layer). In addition, it is very difficult to distinguish this information from  
 325 remote sensors because there is a mixture of new small particles combined with the larger  
 326 particles that are growing and eventually fall faster than the updrafts. This is consistent with  
 327 the results from our model studies, where ice activates quickly and then is efficiently mixed  
 328 with snow in the mixed-phase cloud layer. This is clearly seen in Figure S1a, where  
 329 ice+snow number concentrations are well-mixed in the cloud layer. Results from these model  
 330 studies, remote sensing of mixed-phase clouds, and in-situ measurements highlight the  
 331 difficulty of determining where ice nucleates in a cloud layer that is well-mixed by turbulent  
 332 eddies. This discussion has been added to Section 4.1.



333  
 334 **Figure S1:** Time-height cross sections of (A) ice+snow number concentration, in units of  $L^{-1}$ ,  
 335 and (B) IN advection plus subsidence, in units of  $L^{-1}hour^{-1}$ , from CNT simulation.  
 336 Temperature, in units of  $^{\circ}C$ , shown with black contour lines.

337

338 A key aspect of the study resides in the IN reservoir formed by the sub-cloud mixed layer.  
339 While SubCL NIN decreases much faster than CL NNI after 10h, it seems that NIN also  
340 increases faster than NNI before 10h in the control run (there is a jump of ~200 mL<sup>-1</sup> for  
341 NIN compared to ~100 mL<sup>-1</sup> for NNI). This looks almost like more IN particles are released  
342 in the sub cloud layer than ice crystals are formed in the cloud. Could you please clarify this  
343 point and explain why sub-cloud NIN increases so rapidly at first? How do the total number  
344 NIN+NNI in the cloud and sub-cloud layers evolves in each case (this could be an addition to  
345 figure 7d)? Also, what is causing the reversal in the integrated NIN trend after 10h while  
346 sublimation fluxes remain roughly constant?

347 The rapid increase in subcloud  $N_{IN}$  is due to the rapid deepening of the mixed-layer (due to  
348 the height of the mixed-layer base) in the first 10 hours, seen Figure 8c. After the first 10  
349 hours the mixed-layer deepens at a slower rate.

350 Looking at Figures 7 & 8, it seems that the simulated clouds in the control and noRecycle  
351 runs are almost identical at the beginning of the analysis period, that is at 6h. Only the IN  
352 flux through cloud base is initially different between the two cases, highlighting the influence  
353 of sub cloud IN recycling. Could you indicate why is recycling apparently so unimportant in  
354 controlling the cloud properties before 6h?

355 This is because the NoRecycle run is started with the Control state at hour 6 in order to  
356 prevent the runs from diverging during spinup. A sentence has been added on page 11734  
357 line 20 which reads, 'The NoRecycle run is started from the Control run at hour 6 to prevent  
358 the two simulations from diverging due to spinup.'. Apologies for leaving this information  
359 out of the first version of the paper.

360 Moreover, on p11738-114/17, it is stated that "the rapid increase in LWP [...] increases the  
361 turbulent mixing of IN from the sub cloud layer into the cloud layer". This statement seems  
362 however to contradict Figure 8b where the IN turbulent fluxes at cloud base are always lower  
363 in noRecycle compared to control.

364 Turbulence is larger in NoRecycle due to the larger LWP but the IN gradients are smaller due  
365 to the rapid depletion of IN, therefore the turbulent flux of IN at cloud base is smaller in  
366 NoRecycle compared to Control. The sentence has been left unchanged.

367 Finally, Figure 8b also shows almost constant sublimation fluxes in the control run during the  
368 whole simulation time. Sublimation should however release water vapor and thus reduce the  
369 sublimation rates and IN recycling. This does not appear to be the case here. How can  
370 sublimation be sustained at nearly constant rates in these conditions, without the sub-cloud  
371 layer becoming saturated with respect to ice? How do ice saturation and the water vapor  
372 mixing ratio evolve in the sub-cloud layer in your simulations? Additional figures showing  
373 the evolution of ice saturation, water vapor mixing ratio and temperature in the sub-cloud  
374 layer might help. More generally, relative humidity in the mixed-layer seems to be the most  
375 important ingredient determining the role of IN recycling in sustained ice production. From  
376 that perspective, how representative is the studied case compared to typical AMPS?

377 Two time-height cross sections of horizontally-averaged relative humidity with respect to ice  
378 and water vapor mixing ratio have been added to the paper in Figure 7c,d. The Figure shows  
379 the continuous drying of the sub-cloud layer due to the dominance of the drying due to the  
380 water vapor flux over the moistening due to sublimation. This is what allows sublimation to  
381 be maintained in the simulations. The consistent drying and cooling of the mixed layer due to  
382 radiative cooling and turbulent mixing in these simulations is fundamental in any AMPS that  
383 is precipitating ice out of the mixed layer and has limited fluxes of water vapor at the mixed  
384 layer base. Of course, if water vapor fluxes at the mixed-layer base increases to the extent  
385 that the mixed layer becomes saturated with respect to ice then recycling will be shut off.

386 **Minor comments and technical corrections:**

387 1. p11728-124: "a liquid layer that precipitates ice crystals" sounds a bit strange. Please  
388 consider rephrasing.

389 The sentence has been rewritten to read, "AMPS are characterized by a liquid cloud  
390 layer with ice crystals that precipitate from cloud base even at temperatures well below  
391 freezing...".

392 2. p11729-120: "mineral dust, soot, sea salts and bacteria", as well as the list of references  
393 given 122-24. Perhaps match the corresponding references with the different IN  
394 compounds, i.e. "mineral dust (Mohler et al., 2006; Welti et al., 2009...), soot (DeMott,  
395 1990...), sea salts (Wise et al., 2012)...".

396 Sentence changed as suggested.

397 3. p11730-122/26: "We posit that recycling plays a significant role more generally since,  
398 for example, assuming an adiabatic vertical profile, a 650 m-deep mixed layer with a  
399 cloud-top temperature of -16C requires a water vapor mixing ratio of at least 1.7 gkg-1  
400 at mixed-layer base to be saturated with respect to ice, i.e. in order for recycling to be a  
401 negligible source of ice nuclei in the mixed layer." The sentence may be slightly too  
402 long. Please consider splitting or rewording it. Besides, isn't it a little bit too strong to  
403 suppose that IN recycling may be significant unless the mixed-layer is saturated with  
404 respect to ice (if I understood correctly the meaning of this sentence)?

405 Yes, this sentence is worded too strongly. We feel the sentence read better as one  
406 sentence and does not need to be split into two sentences. The wording has been  
407 rewritten to read, "We posit that recycling may make IN available for nucleation more  
408 generally since,...".

409 4. p11731-124/26: "a cloud layer extending into the inversion by 100 m, cloud base at 0.9  
410 km, and cloud top at 1.5 km." How stable were these conditions? How did the cloud  
411 boundaries evolve in time according to the radar retrievals? How long did the AMPS  
412 persist over Barrow?

413 This sentence has been changed to read, “Measurements from ground-based, vertically  
414 pointing, 35-GHz cloud radar, micropulse lidar, and dual-channel microwave radiometer  
415 at Barrow indicated a mixed-phase cloud layer starting at 8UTC on 8 April 2008 with a  
416 cloud top at approximately 1.5km that slowly descended to approximately 0.5 km over a  
417 26 hour period. At the time of the 17:34 sounding the cloud layer extended into the  
418 inversion by 100 m, had a cloud base at 0.9 km, and cloud top at 1.15 km.”

419 5. p11732-110: How was the average value of 0.4 L-1 calculated based on the 2D-S and  
420 2D-P probes? Is it an average from the two devices, or were data from 2D-S and 2D-P  
421 for different size ranges combined?

422 The data from the 2D-S and 2D-P were averaged to together to get an average number  
423 concentration. The sentence has been reworded to read, “Ice crystal number  
424 concentrations measured by Stratton Park Engineering Company 2D-S and Particle  
425 Measuring Systems 2D-P optical array probes for sizes larger than 100 mm together  
426 averaged 0.4 L<sup>-1</sup>.”

427 6. p11732-124: How was this particular value of the divergence (2.5ex10-6 s-1) selected?  
428 What about the initial surface pressure and surface fluxes?

429 The section on the divergence has been changed to read, “Divergence is assumed to be  
430  $2.5 \times 10^{-6} \text{ s}^{-1}$  below the temperature inversion and zero above, giving a linear increase in  
431 large-scale subsidence from zero at the surface to  $2.7 \text{ mms}^{-1}$  at the base of the initial  
432 inversion ( $z = 1.1 \text{ km}$ ). This value for divergence was chosen so that the height of the  
433 temperature inversion at cloud top is steady. The divergence used in this study is smaller  
434 than the divergence used in the WRFLES study of the same case by Solomon et al.  
435 (2014) due to the reduced LWPs in this current study and therefore reduced turbulent  
436 entrainment that balances large-scale subsidence in a steady simulation.” In addition, the  
437 sentence, “Initial surface pressure is 1020 hpa.” has been added before the description of  
438 divergence.

439 Additional details have been added about the surface layer scheme, “Surface fluxes are  
440 calculated uses the modified MM5 similarity scheme with calculates surface exchange  
441 coefficients for heat, moisture, and momentum following Webb (1970) and uses Monin-  
442 Obukhov with Carlson-Boland viscous sub-layer and standard similarity functions  
443 following Paulson (1970) and Dyer and Hicks (1970).”

444 7. p11734-112/23: I would suggest moving the paragraph at the end of the section, i.e. after  
445 the description of the IN/recycling parameterization.

446 The paragraph has been moved to after the description of the IN/recycling  
447 parameterization.

448 8. p11736-16/7: If I am correct, 5.8 L-1 is the TOTAL IN concentration, i.e. the sum of the  
449 NIN in each bin. Maybe this should be specified. Also, it could be interesting to have an  
450 idea of the NIN distribution with respect to the threshold temperature. You could for  
451

452 example indicate what the IN concentration within the first and last bins is. Besides, is  
453 there any particular treatment required for the first bin as it includes all the particles  
454 active between -15.5C and 0C? Is it correct and realistic to say that all the IN within the  
455 first bin spontaneously nucleate ice as soon as water saturation is reached, i.e. at cloud  
456 base?

457 Page 11736 lines 4-5 have been changed to read, "...an initial  $N_{IN}$  summed over all bins  
458 at every gridpoint equal to  $5.8 \text{ L}^{-1}$ ..." Also, at line 6 a discussion has been added  
459 regarding initial  $N_{IN}$  in each bin, "In a discrete bin formulation this results in  $3.26 \text{ L}^{-1}$  in  
460 the warmest bin and  $0.23 \text{ L}^{-1}$  additional IN that are available for nucleation in the coldest  
461 bin. Given the initial temperatures in the cloud layer, all IN from the first bin in the  
462 cloud layer nucleate. This causes an initial spike in cloud ice number concentration,  
463 which also causes a large precipitation flux out of the mixed layer. It takes  
464 approximately 6 hours for the cloud layer to reach a quasi-equilibrium with steady cloud  
465 ice production."

466 9. p11736-123: Is it a liquid or a mixed-phase cloud layer?

467 "liquid" has been changed to "mixed-phase".

468 10. p11737-12 (and whole text): Notations " $N_{NI}$ " (number of ice crystals) and " $N_{IN}$ " (number  
469 of IN) can be easily confused. Perhaps a different notation for the number of ice crystals  
470 could be used.

471 Yes, this is confusing. " $N_{NI}$ " and " $T_{NI}$ " have been changed to " $N_{ICE}$ " and " $T_{ICE}$ " to clearly  
472 distinguish from " $N_{IN}$ " and " $T_{IN}$ ".

473 11. p11740-Equation 7 and p11741-Equation 8b: Perhaps change the notation and add a  
474 subscript to  $f$  to distinguish between cloud base and mixed-layer base values. Also  
475 describe more clearly what allows you to transform equation 8b into 8c.

476 Thank you but we think the notation for  $f$  is clear and does not need a subscript. To  
477 clarify the steps that allow for the transform between eqs. 8b and 8c, "...and since  
478  $f|_{\text{Mixed-Layer Base}}$  is downward and  $f|_{\text{Mixed-Layer Top}}$  is negligible (eq. 5), ..." has been  
479 added between eqs. 8b and 8c.

480 12. p11741-118: "In SW": please rephrase to introduce more clearly the sentence (maybe "in  
481 the presence of short wave radiation", is it what you mean?).

482 The sentence has been changed to read, "In the presence of shortwave radiation (i.e., in  
483 the SW simulation),..."

484 13. p11741: The analysis does not account for any water vapor flux. Sublimation releases  
485 water vapor in the sub-cloud layer, and vapor is also transported through the mixed-layer  
486 boundaries by turbulence. With the water vapor content possibly increasing in the sub-  
487 cloud layer, we may expect the sublimation flux to decrease. How would this be

488 reflected in the simple mixed-layer model, and what would happen in case of a saturated  
489 mixed-layer with respect to ice?

490 A saturated mixed-layer with no sublimation does not change the mixed-layer analysis  
491 presented in Section 5. However, from eq 8c using the same assumptions of  
492  $f|_{\text{Mixed-Layer Base}}$  is downward and  $f|_{\text{Mixed-Layer Top}}$  is negligible, when  $S=0$ ,

$$T_{IN}|_{\text{Mixed-Layer Base}} < T_{IN}|_{\text{Cloud Base}}$$

493 causing IN to be depleted in the mixed layer since entrainment at cloud top is weak.

494 Also, see the two time-height cross sections of horizontally-averaged relative humidity  
495 with respect to ice and water vapor mixing ratio that have been added to the paper in  
496 Figure 7c,d. The Figure shows the continuous drying of the sub-cloud layer due to the  
497 dominance of the drying due to the water vapor flux over the moistening due to  
498 sublimation.

499 14. p11741-end of page: Please provide a short summary of the main implications for actual  
500 AMPS clouds, and for the conditions under which IN recycling is relevant.

501 This discussion has been added at the end of page 11741, “This mixed-layer analysis  
502 provides a framework to understand the results presented in Section 4. Specifically,  
503 sublimation being less than the turbulent flux of IN is seen to be a property of a well-  
504 mixed layer where the total flux at mixed-layer base is downward and the total flux at  
505 the mixed layer top is negligible. In the case where the mixed layer is saturated with  
506 respect to ice, sublimation is equal to zero and the turbulent flux of IN at the mixed-layer  
507 base is less than the turbulent flux of IN at the cloud base, reducing the flux of IN into  
508 the cloud layer. The relationships outlined in this section are appropriate for any AMPS  
509 with weak entrainment at cloud top, weak large-scale advective fluxes, and net  
510 downward fluxes at the mixed-layer base.”.

511 15. p11742-13: If I understand correctly, the start of the green arrow corresponds to sunrise,  
512 the tip of the blue arrow corresponds to maximum SW, and the tip of the red arrow  
513 corresponds to sunset. Am I right? It looks actually like the moon and sun symbols on  
514 Figure 11761 are not absent in the manuscript.

515 The start of the green arrow corresponds to maximum SW (see Figure 11b). The arrows  
516 are used as a means to refer to transitions in the cloud mixed-layer properties. Again,  
517 apologies for the missing symbols. It must have been a challenge to review this paper  
518 with incomplete figures and we appreciate the effort that you have gone to to understand  
519 the results of this study.

520 16. p11742-15/7: What causes the relative humidity to be low at this time? More generally,  
521 what causes the simulated RH cycle despite continuous sublimation and surface  
522 decoupling? Besides, what happens to the precipitation flux at this time?

523 When incoming solar radiation is at a maximum, LWP is at a minimum, which causes  
524 turbulent mixing to be at a minimum. Also, the cloud layer and mixed layer warm,  
525 causing less ice production and less precipitation into the subcloud layer. The warming  
526 of the subcloud layer together with the reduction in precipitation causes the relative  
527 humidity to be at a minimum.

528 17. p11742-123/24: An increase in in-cloud ice concentrations could enhance the  
529 precipitation fluxes in the sub-cloud layer and may dominate over the decrease in  
530 downward turbulent NI flux. Why isn't it the case here? More generally, the role of  
531 precipitation should be more specifically stressed in section 6. To complement the  
532 discussion, it may also be interesting to compare the states at the beginning and at the  
533 end of a full diurnal cycle (Figure 11 shows only a 20h cycle).

534 We actually do say here that both IWP and precipitation increase when incoming solar  
535 radiation is a minimum. There is a net downward flux of NI out of the cloud layer. This  
536 discussion was just meant to point out that turbulence acts against this downward flux.  
537 Figure 11 shows a 24-hour cycle, the red arrow only extends to hour 62 and the green  
538 arrow begins at hour 42, while the cycle is for the 40-64 hour period.

539 18. p11743-12: Sub-cloud drying has not been mentioned earlier in the study, and Figure 11  
540 does not seem to confirm that. A figure showing the evolution of below cloud humidity  
541 in the control and SW runs would be very instructive. Again referring to my main  
542 comment, relative humidity in the mixed-layer is a key ingredient controlling IN  
543 recycling via sublimation. Can you please comment on this and stress the relevance of  
544 the case study presented compared to typical AMPS.

545 Two time-height cross sections of horizontally-averaged relative humidity with respect  
546 to ice and water vapor mixing ratio have been added to the paper in Figure 7c,d. The  
547 Figure shows the continuous drying of the sub-cloud layer due to the dominance of the  
548 drying due to the water vapor flux over the moistening due to sublimation. Fig. 7 also  
549 shows the time-height cross sections of horizontally-averaged water vapor mixing ratio  
550 and relative humidity with respect to ice. This brief discussion has been added at the end  
551 of the second paragraph in Section 4, "Fig. 7 also shows the time-height cross sections of  
552 horizontally-averaged water vapor mixing ratio and relative humidity with respect to ice.  
553 These figures show that the continuous drying and cooling of the mixed layer results in  
554 continuous sublimation in the subcloud layer."

555 19. Figure 1: The grey shadings do not appear clearly or are absent.

556 There seems to have been a problem with the figures in the online version of the paper.  
557 I'm sorry I didn't catch this before the paper was sent out for review. All the figures are  
558 complete in the revised paper.

559 20. Figure 3: Could you please add a legend and axis labels to the figure?



560 I'm sorry, I don't know why the legends and labels were removed from the online  
561 version of the paper. We will make sure the revised version is correct.

562 21. Figure 4: In the caption, I guess that the second sentence refers to figure c).

563 The figure caption has been reworded for clarity, "A,B,D) Sensitivity of LWP and IWP  
564 to snow density and fall speeds. LWP shown with solid lines and IWP shown with  
565 dashed lines, in units of  $\text{g m}^{-2}$ . C) Fall speeds used in sensitivity studies, in units of  $\text{m s}^{-1}$ ....".  
566

567 22. Figure 7, 8 & 10: The horizontal axis labels and titles are missing.

568 Our apologies for this. The labels and titles were removed in the online version for some  
569 reason. We have added the labels and titles back in and will insure that the revised online  
570 version is complete.

571 The Role of Ice Nuclei Recycling in the Maintenance of Cloud Ice in

572 Arctic Mixed-Phase Stratocumulus

573 Amy Solomon<sup>12</sup>, Graham Feingold<sup>2</sup>, and Matthew D. Shupe<sup>12</sup>

574 (1) Cooperative Institute for Research in Environmental Sciences, University of Colorado

575 Boulder, Boulder, Colorado, USA.

576 (2) Earth System Research Laboratory, National Oceanic and Atmospheric Administration,

577 Boulder, Colorado, USA.

578

579 Corresponding author: Amy Solomon, NOAA/ESRL, PSD3, 325 Broadway, Boulder,

580 Colorado 80305-3337, USA. (amy.solomon@noaa.gov)

581 | [July 31, 2015](#)

582

### Abstract

583 This study investigates the maintenance of cloud ice production in Arctic mixed phase  
584 stratocumulus in large eddy simulations that include a prognostic ice nuclei (IN) formulation  
585 and a diurnal cycle. Balances derived from a mixed-layer model and phase analyses are used  
586 to provide insight into buffering mechanisms that maintain ice in these cloud systems. We  
587 find that for the case under investigation, IN recycling through subcloud sublimation  
588 considerably prolongs ice production over a multi-day integration. This effective source of  
589 IN to the cloud dominates over mixing sources from above or below the cloud-driven mixed  
590 layer. Competing feedbacks between dynamical mixing and recycling are found to slow the  
591 rate of ice lost from the mixed layer when a diurnal cycle is simulated. The results of this  
592 study have important implications for maintaining phase partitioning of cloud ice and liquid  
593 that determine the radiative forcing of Arctic mixed-phase clouds.

Amy Solomon NOAA 7/20/2015 4:32 PM  
Deleted: -

595 **1 Introduction**

596 Reliable climate projections require realistic simulations of Arctic cloud feedbacks. Of  
597 particular importance is accurately simulating Arctic mixed-phase stratocumuli (AMPS),  
598 which are ubiquitous and play an important role in regional climate due to their impact on the  
599 surface energy budget and atmospheric boundary layer structure through cloud-driven  
600 turbulence, radiative forcing, and precipitation (Curry et al., 1992; Walsh and Chapman,  
601 1998; Intrieri et al., 2002; Shupe and Intrieri, 2004; Sedlar et al., 2011; Persson, 2012). For  
602 example, Bennartz et al. (2012) showed that the extreme melt events observed at Summit,  
603 Greenland in July 2012 would not have occurred without the surface radiative forcing  
604 produced by AMPS.

605 AMPS are characterized by a liquid cloud layer with ice crystals that precipitate from cloud  
606 base even at temperatures well below freezing (Hobbs and Rangno, 1998; Intrieri et al.,  
607 2002; McFarquhar et al., 2007). Radiative cooling near cloud top generates turbulence that  
608 maintains the liquid layer and forms an approximately well-mixed layer that extends as far as  
609 500 meters below cloud base. These cloud-driven mixed layers are frequently decoupled  
610 from the surface layer, limiting the impact of fluxes of heat, moisture, and aerosols on the  
611 cloud layer from below (Solomon et al., 2011; Shupe et al., 2013). However, unlike  
612 subtropical cloud-topped boundary layers where decoupling enhances cloud breakup by  
613 cutting the cloud system off from the surface source of moisture, decoupled AMPS can  
614 persist for extended periods of time due to weak precipitation fluxes out of the mixed layer  
615 and relatively moist air entrained into the cloud layer at cloud top (Tjernström et al., 2004;  
616 Solomon et al., 2011; Sedlar et al., 2012; Solomon et al., 2014).

Amy Solomon 7/23/2015 3:29 PM

Deleted: that

Amy Solomon 7/23/2015 3:38 PM

Deleted: precipitates

619 AMPS are challenging to model due to uncertainties in ice microphysical processes that  
620 determine phase partitioning between ice and radiatively important cloud liquid water  
621 (Sandvik et al., 2007; Tjernström et al., 2008; Klein et al., 2009, Karlsson and Svensson,  
622 2011; Barton et al., 2012; Birch et al., 2012; de Boer et al., 2012), which drives turbulence  
623 that maintains the system. Phase partitioning depends upon the number, shape, and size of ice  
624 crystals, since these determine the efficiency of water vapor uptake by ice and hence the  
625 availability of water vapor for droplet formation (Chen and Lamb, 1994; Sheridan et al.,  
626 2009; Ervens et al., 2011; Hoose and Möhler, 2012).

627 Since temperatures in AMPS are too warm for homogenous ice nucleation, ice must form  
628 through heterogeneous nucleation. Aerosols with properties to serve as seeds for  
629 heterogeneous ice crystal formation are referred to as ice nuclei (IN). A number of different  
630 aerosols such as mineral dust ([Broadley et al., 2012](#); [Kulkarni et al., 2012](#); [Lüönd et al., 2010](#);  
631 [Möhler et al. 2006](#); [Pinti et al., 2012](#); [Welti et al., 2009](#)), soot ([DeMott, 1990](#)), sea salts ([Wise  
632 et al., 2012](#)), and bacteria ([Kanji et al., 2011](#); [Levin and Yankofsky, 1983](#)) have been  
633 observed to act as IN, all of which nucleate at different temperatures and supersaturation  
634 ranges. In addition, observations indicate that nucleation properties are modified by aging  
635 and coating of aerosols ([Möhler et al., 2005](#); [Cziczo et al. 2009](#)). Heterogeneous ice  
636 nucleation can occur by a number of modes: either in the presence of super-cooled droplets,  
637 when an aerosol comes into contact with a droplet (contact freezing), is immersed in a  
638 droplet (immersion freezing), or by vapor deposition on IN (deposition freezing) ([Pruppacher  
639 and Klett, 1997](#)).

Amy Solomon NOAA 7/20/2015 4:29 PM  
Deleted: -

641 IN can be entrained into the cloud-driven mixed layer through turbulent mixing from above  
642 and/or below. Recent studies indicate that entrainment alone cannot account for observed ice  
643 crystal number concentration ( $N_{ICE}$ ) (Fridlind et al., 2012), motivating the use of diagnostic  
644 formulations for ice formation to produce model simulations of AMPS with realistic phase  
645 partitioning (Ovchinnikov et al., 2011). While this modeling strategy constrains  $N_{ICE}$  to be  
646 close to the measured values it eliminates the dynamical-microphysical feedbacks that  
647 regulate ice/liquid phase partitioning (Avramov et al., 2011).

Amy Solomon 7/29/2015 6:01 PM

Deleted: N

Amy Solomon 7/29/2015 6:01 PM

Deleted: N

648 Here we investigate a relatively unexplored source of ice production--recycling of ice  
649 nuclei in regions of ice subsaturation. AMPS frequently have ice-subsaturated air near the  
650 cloud-driven mixed-layer base where falling ice crystals can sublimate, leaving behind IN.  
651 This feedback loop is referred to hereon as "recycling". Recycling was found to be  
652 significant in large eddy simulations of a single-layer stratocumulus observed during the  
653 Department of Energy, Atmospheric Radiation Measurement Program's Mixed-Phase Arctic  
654 Cloud Experiment (M-PACE; Verlinde et al., 2007; Fan et al., 2009). AMPS observed during  
655 M-PACE formed due to a cold-air outbreak, where large fluxes of heat and moisture over the  
656 open ocean forced turbulent roll clouds that were coupled to the surface layer. This coupling  
657 with the surface layer prevented the identification of the role of dynamics internal to the  
658 cloud-driven mixed layer in maintaining phase-partitioning.

Amy Solomon NOAA 7/20/2015 4:35 PM

Deleted: .O.E.

659 In this study we focus on the internal microphysics and dynamics of the cloud-driven mixed  
660 layer by investigating processes in an AMPS decoupled from surface sources of moisture,  
661 heat, and ice nuclei. We posit that recycling plays a significant role more generally since, for  
662 example, assuming an adiabatic vertical profile, a 650 meter-deep mixed layer with a cloud-

666 top temperature of  $-16^{\circ}\text{C}$  requires a water vapor mixing ratio of at least  $1.7\text{ g kg}^{-1}$  at mixed-  
667 layer base to be saturated with respect to ice, i.e., in order for recycling to be a *negligible*  
668 source of ice nuclei in the mixed layer. This value is typically only seen in the Arctic  
669 between May-September (Serreze et al., 2012), while persistent AMPS frequently occur  
670 outside of these months (Shupe et al., 2011).

671 We examine the role of IN recycling in maintaining ice production using large eddy  
672 simulations of a springtime decoupled AMPS. Three simulations are analyzed; a “Control”  
673 with recycling turned on and shortwave radiation turned off (to compare with previous  
674 simulations of this case that use different IN formulations and shortwave radiation turned off),  
675 “NoRecycle” with IN recycling turned off to identify the impact of recycling on the cloud  
676 life-time and phase partitioning, and “SW” with recycling and shortwave radiation turned on  
677 to identify the impact of realistic diurnal heating and cooling tendencies on the recycling  
678 process. This study builds on previous studies of this case, all of which exclude shortwave  
679 radiation (Avramov et al., 2011; Solomon et al., 2011, 2014), by including a prognostic  
680 equation for IN and a diurnal cycle. Within this modeling framework we investigate the  
681 relative roles of recycling and entrainment of IN in maintaining cloud ice production.

## 682 2 Case Description

683 The case derives from observations of a persistent single-layer Arctic mixed-phase  
684 stratocumulus cloud observed near Barrow, AK on 8 April 2008 during the Indirect and  
685 Semi-Direct Aerosol Campaign (McFarquhar et al., 2011) (see Fig. 1). The adjacent Beaufort  
686 Sea was generally ice covered during this time, with significant areas of open water observed  
687 east of Barrow. A 4-K temperature inversion with inversion base at 1.05 km was observed

Amy Solomon NOAA 7/20/2015 2:36 PM

**Deleted:** with shortwave radiation turned off to compare with previous simulations of this case that use different IN formulations

Amy Solomon 7/29/2015 3:36 PM

**Deleted:** ure

692 via a radiosonde at 17:34UTC; static stability was near neutral within the mixed layer  
693 overlaying a stable near-surface layer with static stability greater than  $2 \text{ K km}^{-1}$  below 500 m.  
694 The water vapor mixing ratio,  $q_v$ , decreased from  $1.7 \text{ g kg}^{-1}$  at the surface to  $1.2 \text{ g kg}^{-1}$  at  
695 cloud top, above which a secondary maximum of  $1.6 \text{ g kg}^{-1}$  was observed. Winds were east-  
696 southeasterly throughout the lowest 2 km.

697 Measurements from ground-based, vertically pointing, 35-GHz cloud radar, micropulse lidar,  
698 and dual-channel microwave radiometer at Barrow indicated a mixed-phase cloud layer  
699 starting at 8 UTC on 8 April 2008 with a cloud top at approximately 1.5km that slowly  
700 descended to approximately 0.5 km over a 26 hour period. At the time of the 17:34 sounding  
701 the cloud layer extended into the inversion by 100 m, had a cloud base at 0.9 km, and cloud  
702 top at 1.15 km. Cloud ice water path (IWP), derived from cloud radar reflectivity  
703 measurements, varied from  $20\text{--}120 \text{ g m}^{-2}$  within 10 min of the sounding, with an uncertainty  
704 of up to a factor of 2 (Shupe et al., 2006). Concurrently liquid water path (LWP), derived  
705 from dual-channel microwave radiometer measurements, was  $39\text{--}62 \text{ g m}^{-2}$ , with an  
706 uncertainty of  $20\text{--}30 \text{ g m}^{-2}$  (Turner et al., 2007).

707 Research flights were conducted by the National Research Council of Canada Convair-580 at  
708 22:27-23:00 UTC on 8 April 2008 over the ocean northwest of Barrow (McFarquhar et al.,  
709 2011). Droplet concentrations measured by a Particle Measuring Systems Forward Scattering  
710 Spectrometer Probe varied between 100 and  $200 \text{ cm}^{-3}$ . Ice crystal number concentrations  
711 measured by Stratton Park Engineering Company 2D-S and Particle Measuring Systems 2D-  
712 P optical array probes for sizes larger than  $100 \mu\text{m}$  together averaged  $0.4 \text{ L}^{-1}$ . IN  
713 concentrations measured with the Texas A&M Continuous Flow Diffusion Chamber varied

Amy Solomon NOAA 7/27/2015 5:04 PM  
Deleted: ing



715 from  $0.1 \text{ L}^{-1}$  to above  $20 \text{ L}^{-1}$ . Ice crystal habit estimated using the automated habit  
716 classification procedure of Korolev and Sussman (2000) indicated primarily dendritic crystal  
717 habits.

### 718 3 Model Description

719 We use the large eddy simulation mode of the Advanced Research WRF model (WRFLES)  
720 Version 3.3.1 (Yamaguchi and Feingold, 2012) with the National Center for Atmospheric  
721 Research Community Atmospheric Model longwave radiation package (Collins et al., 2004),  
722 RRTMG shortwave package (Iacono et al., 2008), the Morrison two-moment microphysical  
723 scheme (Morrison et al., 2009), and a 1.5-order turbulent kinetic energy prediction scheme  
724 (Skamarock et al., 2008). Surface fluxes are calculated uses the modified MM5 similarity  
725 scheme with calculates surface exchange coefficients for heat, moisture, and momentum  
726 following Webb (1970) and uses Monin-Obukhov with Carlson-Boland viscous sub-layer  
727 and standard similarity functions following Paulson (1970) and Dyer and Hicks (1970).

728 All model runs are initialized with winds, temperature, and water vapor from the 17Z 8 April  
729 2008 sounding at Barrow, AK (see Fig.1). Initial surface pressure is 1020 hPa. Divergence is  
730 assumed to be  $2.5 \times 10^{-6} \text{ s}^{-1}$  below the temperature inversion and zero above, giving a linear  
731 increase in large-scale subsidence from zero at the surface to  $2.7 \text{ mm s}^{-1}$  at the base of the  
732 initial inversion ( $z=1.1 \text{ km}$ ). This value for divergence was chosen so that the height of the  
733 temperature inversion at cloud top is steady. The divergence used in this study is smaller than  
734 the divergence used in the WRFLES study of the same case by Solomon et al. (2014) due to

Amy Solomon NOAA 7/20/2015 4:32 PM  
Deleted: -

Amy Solomon NOAA 7/27/2015 3:57 PM  
Deleted: a Monin-Obukhov surface layer (Paulson, 1970),

Amy Solomon 7/28/2015 10:05 PM  
Deleted: Figure

739 | the reduced LWPs in this current study and therefore reduced turbulent entrainment that  
740 | balances large-scale subsidence in a steady simulation.

741 | All simulations are run on a domain of  $3.2 \times 3.2 \times 1.8$  km with a horizontal grid spacing of  
742 | 50 m and vertical spacing of 10 m. The domain has  $65(x) \times 65(y) \times 180(z)$  gridpoints and is  
743 | periodic in both the x- and y-directions. The top of the domain is at 1.8 km, which is 0.7 km  
744 | above cloud top in this case. The model time step is 0.75 s. The structure of the cloud layer is  
745 | insensitive to changes in resolution and domain size. For example, tests run for Solomon et al.  
746 | (2014) demonstrated that increasing the vertical and horizontal resolutions by a factor of two  
747 | resulted in an increase in LWP and IWP by 5% and 1%, respectively, while increasing the  
748 | domain size by a factor of two in both the x- and y-directions results in an increase in LWP  
749 | and IWP of less than 1%.

750 | Cloud droplets are activated using resolved and subgrid vertical motion (Morrison and Pinto  
751 | 2005) and a log-normal aerosol size distribution (assumed to be ammonium bisulfate and  
752 | 30% insoluble by volume) to derive cloud condensation nuclei spectra following Abdul-  
753 | Razzak and Ghan (2000). The aerosol accumulation mode is specified with concentrations of  
754 |  $165 \text{ cm}^{-3}$ , modal diameter of  $0.2 \mu\text{m}$ , and geometric standard deviation of  $1.4 \mu\text{m}$ , based on in  
755 | situ ISDAC measurements. In this formulation, IN and cloud condensation nuclei are treated  
756 | as separate species.

757 | Temperature and moisture profiles are nudged to the initial profiles in the top 400 m of the  
758 | domain with a time scale of 1 hour. The model is initialized with winds, temperature, and  
759 | water vapor similar to the Control integration from Solomon et al. (2014). Horizontal winds

760 are nudged to the initial profiles at and above the initial inversion base with a timescale of 2  
761 hours. Initial temperature and subgrid turbulent kinetic energy (TKE) are perturbed below the  
762 top of the mixed layer with pseudo-random fluctuations with amplitudes of +/- 0.1 K and 0.1  
763  $\text{m}^2 \text{s}^{-2}$ , respectively. The liquid layer is allowed to form in the absence of ice during the first  
764 hour of the integration to prevent potential glaciation during spinup.

765 The cloud-driven mixed layer is defined as the region where the liquid-ice water static energy  
766 is approximately constant with height. We define the boundaries of the mixed-layer top and  
767 base to occur where the slopes of liquid-ice static energy exceed  $7 \times 10^{-3} \text{ K m}^{-1}$  and  $1 \times 10^{-3} \text{ K}$   
768  $\text{m}^{-1}$ , respectively. Cloud top and base are defined as the heights where cloud water mixing  
769 ratio,  $q_c$ , is equal to  $1 \times 10^{-4} \text{ g kg}^{-1}$ .

770 Nested Weather Research and Forecasting (WRF) model simulations of this case performed  
771 with an inner grid at LES resolution (Solomon et al. 2011) demonstrate that moisture is  
772 provided to the cloud system by a total water inversion at cloud top and that the mixed layer  
773 does not extend to the surface, i.e., the mixed layer is largely decoupled from surface sources  
774 of moisture. In addition, the nested simulations indicate that cloud liquid water,  $q_c$ , is  
775 maintained within the temperature inversion by downgradient turbulent fluxes of  $q_v$  from  
776 above and direct condensation driven by radiative cooling. These processes cause at least  
777 20% of  $q_c$  to extend into the temperature inversion.

778 WRFLES has been modified to include a prognostic equation for IN number concentration  
779 ( $N_{IN}$ ),

Amy Solomon NOAA 7/20/2015 4:37 PM

Deleted: s

Amy Solomon NOAA 7/20/2015 4:40 PM

Deleted: water vapor mixing ratio

$$\frac{\partial N_{IN}}{\partial t} + ADV + DIFF = \left. \frac{\delta N_{IN}}{\delta t} \right|_{activation} + \left. \frac{\delta N_{IN}}{\delta t} \right|_{sublimation} \quad (1)$$

782 where ADV represents advection and DIFF represents turbulent diffusion. Activation is also  
 783 referred to as nucleation of ice and sublimation is also referred to as recycling of IN.

784 Here we adopt an empirical approach by initializing  $N_{IN}$  with an observationally based  
 785 relationship expressing the number of available IN as a function of temperature in regions of  
 786 water-saturation (DeMott et al., 2010),

$$N_{IN} = F * 0.117 \exp(-0.125 * (T - 273.2)) \quad (2)$$

787 where F is an empirically derived scale factor and T is temperature in Kelvin. Sixteen  
 788 prognostic equations are integrated for  $N_{IN}$  in equally spaced temperature intervals with  
 789 nucleation thresholds between -20.2°C and -15.5°C (see Fig. 2). Therefore, additional IN  
 790 become available for activation as the cloud layer cools. Initial  $N_{IN}$  concentrations are a  
 791 function of the nucleation threshold temperatures and are independent of the in-situ  
 792 temperature. The in-situ temperature in regions of water saturation determines how many IN  
 793 are activated. To take deviations from the empirical derivation into account, IN are activated  
 794 with 50% efficiency (by multiplying the activation tendency in equation (1) by 0.5), however  
 795 results are insensitive to this parameter (not shown). Due to the pristine dendritic nature of  
 796 the observed crystals, ice shattering and aggregation are neglected in the simulations and  
 797 sublimation returns one  $N_{IN}$  per crystal.

798  $N_{IN}$  (in units of  $L^{-1}$ ) integrated over the domain in each temperature bin  $k$  at time  $t$  is equal to

Amy Solomon 7/28/2015 10:04 PM

Deleted: ure

$$\bar{N}_{IN}(k, t) = \iiint N_{IN}(x, y, z, k, t) dx dy dz. \quad (3)$$

800 Upon sublimation, the modification of activation thresholds that can occur for previously  
 801 nucleated IN, i.e. preactivation (Roberts and Hallett, 1967), is not considered and  $N_{IN}$  are  
 802 returned to each bin  $k$  with weighting

$$W_k = [\bar{N}_{IN}(k, 0) - \bar{N}_{IN}(k, t)] / \bar{N}_{IN}(k, 0) \quad (4)$$

803 where  $W_k$  is normalized such that  $\sum W_k = 1$ . The  $W_k$  are recalculated each time step. In this  
 804 way, IN are recycled preferentially to each of the 16 temperature bins from which they  
 805 originated (Feingold et al., 1996).

806 The factor F in Eq. (2) is set to 4 for all simulations yielding an initial  $N_{IN}$  summed over all  
 807 bins at every gridpoint equal to  $5.8 \text{ L}^{-1}$ , compared to  $10 \text{ L}^{-1}$  used in LES studies of the same  
 808 case presented in Avramov et al. (2011). In a discrete bin formulation this results in  $3.26 \text{ L}^{-1}$   
 809 in the warmest bin and  $0.23 \text{ L}^{-1}$  additional IN that are available for nucleation in the coldest  
 810 bin. Given the initial temperatures in the cloud layer, all IN from the first bin in the cloud  
 811 layer nucleate. This causes an initial spike in cloud ice number concentration, which also  
 812 causes a large precipitation flux out of the mixed layer. It takes approximately 6 hours for the  
 813 cloud layer to reach a quasi-equilibrium with steady cloud ice production. Supplementary  
 814 integrations were done to test for robustness of the results presented in Section 4 by varying  
 815 initial IN concentrations, i.e., the factor F, (shown in Fig. 3) and by varying snow density and  
 816 fall speeds (shown in Fig. 4). Fig. 3 shows that the simulation maintains ice production when  
 817 the initial  $N_{IN}$  is increased or decreased by  $\sim 3 \text{ L}^{-1}$  relative to Control. Fig. 4 shows that the

Amy Solomon 7/28/2015 10:04 PM  
 Deleted: ure  
 Amy Solomon 7/28/2015 10:05 PM  
 Deleted: ure  
 Amy Solomon 7/28/2015 10:04 PM  
 Deleted: ure  
 Amy Solomon 7/28/2015 10:04 PM  
 Deleted: ure

822 simulations maintain quasi-steady ice and liquid water paths after an initial spinup but the  
823 amount of ice produced is sensitive to the snow fall speed.

824 Crystal size distributions for averaged values of ice water mixing ratio and number  
825 concentration from the Control integration are shown in Fig. 5. These crystal size  
826 distributions are consistent with the Avramov et al. (2011) simulations of this case where  
827 crystal habits are assumed to be high-density pristine dendrites. The distribution shown in Fig.  
828 5 underestimates the number of large (greater than 5mm) crystals as estimated by the 2D-S  
829 and 2D-P probes (see Avramov et al. (2011) for a detailed discussion of the measurements).

830 The Control integration is run with shortwave radiation turned off in order to compare with  
831 previous LES studies of this case (Avramov et al. 2011; Solomon et al. 2014). The results of  
832 Control are compared to two additional simulations; one with IN recycling turned off  
833 (hereafter “NoRecycle”) and one with recycling and shortwave radiation both turned on  
834 (hereafter “SW”). SW is used to investigate how the diurnal cycle impacts IN recycling and  
835 ice formation. All runs use the same setup except SW has subsidence reduced by 30% to  
836 keep the mixed-layer top from lowering appreciably because of smaller LWPs. This allows  
837 for direct comparisons of mixed layer structure and fluxes at the mixed layer boundaries. The  
838 NoRecycle run is started from the Control run at hour 6 to prevent the two simulations from  
839 diverging due to spinup. The first six hours of integration are not used in the analysis to allow  
840 for the spinup of cloud ice. Hours 6-40 are used for analysis of the Control and NoRecycle  
841 simulations and hours 16-76 are used for analysis of the SW simulation to allow for multiple  
842 diurnal cycles.

#### 843 4 Model Results

Amy Solomon 7/28/2015 10:04 PM

Deleted: ure

Amy Solomon 7/29/2015 7:49 PM

Deleted:

Amy Solomon 7/28/2015 10:04 PM

Deleted: ure

Amy Solomon 7/23/2015 4:05 PM

Deleted: .

848 **4.1 Control Integration**

849 In the quasi-steady Control integration, the mixed-layer depth is approximately 850 m and  
850 comprises a 375 m deep mixed-phase cloud layer (henceforth “the cloud layer”), extending  
851 above the mixed-layer top by 25 m, and a 500 m subcloud layer below (Fig. 6). IN are  
852 produced by sublimation of ice crystals below the cloud layer, advected to the cloud layer by  
853 turbulence, and activated as ice crystals (Fig. 6). Ice that forms in the cloud layer is  
854 transported vertically by turbulence, precipitates to cloud base and below, and sublimates  
855 below the cloud layer. At the mixed-layer base, an increase in  $N_{ICE}$  due to precipitation  
856 approximately balances a decrease in  $N_{ICE}$  due to sublimation. These processes constitute a  
857 feedback through which ice production and IN recycling are closely related. This feedback  
858 between ice production and IN in the mixed layer is linked to dynamic-thermodynamic  
859 tendencies, which sustain a subsaturated subcloud layer because the decrease in relative  
860 humidity due to an upward turbulent vapor flux exceeds the increase due to sublimation.

861 The time evolution of horizontally-averaged IN advection plus subsidence (Fig. 7a) shows  
862 that the majority of IN activate at cloud base, which is a bit warmer than cloud top but is  
863 sufficiently cold to activate many of the IN. However, IN from bins with colder threshold  
864 temperatures are advected higher into the cloud where they activate at their threshold  
865 temperature. A secondary maximum is seen at cloud top where the coldest temperatures are  
866 found. Also, it is seen that IN are advected into the cloud layer at cloud top for the first 15-18  
867 hours, but this source of IN decreases as IN in the upper entrainment zone are depleted. The  
868 turbulent mixing of snow and ice in the mixed-phase cloud layer is clearly seen in Fig. 7b,  
869 where ice plus snow number concentrations are well-mixed in the cloud layer. Given the

- Amy Solomon 7/23/2015 4:08 PM  
Deleted: liquid
- Amy Solomon 7/28/2015 10:03 PM  
Deleted: ure
- Amy Solomon 7/28/2015 10:03 PM  
Deleted: 6
- Amy Solomon 7/28/2015 10:03 PM  
Deleted: ure
- Amy Solomon 7/28/2015 10:03 PM  
Deleted: 6
- Amy Solomon 7/29/2015 6:03 PM  
Deleted: N
- Amy Solomon 7/29/2015 6:12 PM  
Deleted: N

877 efficient mixing by the turbulent eddies, it is not possible to identify whether ice has  
878 nucleated at cloud base or cloud top from the ice number concentrations alone. Fig. 7 also  
879 shows the time-height cross sections of horizontally-averaged water vapor mixing ratio and  
880 relative humidity with respect to ice. These figures show that the continuous drying and  
881 cooling of the mixed layer results in continuous sublimation in the subcloud layer.

882 LWP and IWP remain steady until hour 16 of the simulation, and decrease slowly thereafter  
883 (solid lines in Fig. 8a). LWP and IWP magnitudes are within the observational estimates for  
884 this case. In addition, the cloud system is sustained over a multi-day period similar to  
885 measurements taken during ISDAC. Continuous cloud-top cooling causes the minimum  
886 horizontally-averaged temperature (near cloud top) to decrease from  $-17.5^{\circ}\text{C}$  to  $-20^{\circ}\text{C}$  from  
887 hour 10 to hour 40 (Fig. 8b).

888 Over the 40-hour integration, the cloud layer remains decoupled from the surface (Fig. 8c).  
889 However, this does not prevent the number concentration of ice crystals ( $N_{ICE}$ ) in the cloud  
890 layer from remaining relatively steady, decreasing from vertically integrated values of 372 to  
891  $365\text{ m L}^{-1}$  (Fig. 8d, or in terms of vertically averaged cloud layer values,  $1.2\text{ L}^{-1}$  to  $1.1\text{ L}^{-1}$ ).  
892 By contrast, while  $N_{ICE}$  is maintained in the cloud layer,  $N_{IN}$  in the subcloud layer decreases  
893 significantly from  $2\text{ L}^{-1}$  to  $0.2\text{ L}^{-1}$  over the same period. Therefore, even though more  $N_{ICE}$   
894 are lost from the cloud than are activated (Fig. 9a), the relatively constant flux of IN into the  
895 cloud layer (Fig. 9b) allows  $N_{ICE}$  in the cloud to decrease at a slower rate than  $N_{IN}$  in the  
896 subcloud layer. The continuous loss of  $N_{IN}$  in the subcloud layer is due to the IN flux into the  
897 cloud layer exceeding the  $N_{IN}$  gained through sublimation and turbulent advection at mixed-

- Amy Solomon 7/28/2015 10:03 PM  
Deleted: ure
- Amy Solomon 7/28/2015 10:03 PM  
Deleted: 7
- Amy Solomon 7/28/2015 10:03 PM  
Deleted: ure
- Amy Solomon 7/28/2015 10:03 PM  
Deleted: 7
- Amy Solomon 7/28/2015 10:03 PM  
Deleted: ure
- Amy Solomon 7/28/2015 10:03 PM  
Deleted: 7
- Amy Solomon 7/29/2015 6:03 PM  
Deleted: N
- Amy Solomon 7/28/2015 10:02 PM  
Deleted: ure
- Amy Solomon 7/28/2015 10:02 PM  
Deleted: 7
- Amy Solomon 7/29/2015 6:03 PM  
Deleted: N
- Amy Solomon 7/29/2015 6:03 PM  
Deleted: N
- Amy Solomon 7/28/2015 10:02 PM  
Deleted: ure
- Amy Solomon 7/28/2015 10:02 PM  
Deleted: 8
- Amy Solomon 7/28/2015 10:02 PM  
Deleted: g
- Amy Solomon 7/28/2015 10:02 PM  
Deleted: ure
- Amy Solomon 7/28/2015 10:02 PM  
Deleted: 8
- Amy Solomon 7/29/2015 6:04 PM  
Deleted: N



915 layer base (Fig. 9b). This loss is not mitigated by entrainment at mixed-layer top, which is  
916 found to be negligible (Fig. 9c), consistent with Fridlind et al. (2011).

917 The feedback loops discussed above are illustrated by the conceptual diagram in Fig. 10,  
918 where any change to one link in the cycle leads to an increase or decrease in ice production.  
919 For example, a decrease in the turbulent advection of  $N_{IN}$  into the cloud layer, slows the  
920 activation of IN, reduces the precipitation flux into the subcloud layer, reducing sublimation  
921 and availability of IN below cloud base. Both dynamics and thermodynamics play a role in  
922 the buffering aspect of these feedback loops since, for example, the slowing of IN activation  
923 in the example above would lead to increased cloud liquid production, cloud-top radiative  
924 cooling, and enhanced turbulent mixing, which would lead to increased transport of IN into  
925 the cloud layer and therefore increased activation of IN.

#### 926 **4.2 Impact of turning off recycling**

927 When IN recycling is turned off, all IN that activate are lost from the system. This results in a  
928 more rapid loss of IN, a decrease in IWP, and a rapid increase in LWP (Fig. 8a,d, dashed  
929 lines), in contrast to the measurements that show a steady liquid layer and consistent ice  
930 production. Increased cloud liquid water when recycling is turned off results in increased  
931 radiative cooling at cloud top, which causes the cloud-driven mixed layer to cool more  
932 rapidly (Fig. 8b). These results demonstrate the importance of IN recycling in regulating  
933 phase partitioning. The rapid increase in LWP increases cloud-generated turbulence via  
934 enhanced radiative cooling and increases the turbulent mixing of IN from the subcloud layer  
935 into the cloud layer, contributing to a more rapid depletion of IN relative to the Control  
936 integration. This process eventually becomes limited due to depletion of IN in the reservoir

Amy Solomon 7/28/2015 10:02 PM  
Deleted: ure  
Amy Solomon 7/28/2015 10:02 PM  
Deleted: 8  
Amy Solomon 7/28/2015 10:02 PM  
Deleted: ure  
Amy Solomon 7/28/2015 10:02 PM  
Deleted: 8  
Amy Solomon 7/28/2015 10:02 PM  
Deleted: ure  
Amy Solomon 7/28/2015 10:02 PM  
Deleted: 9

Amy Solomon 7/28/2015 10:01 PM  
Deleted: ure  
Amy Solomon 7/28/2015 10:01 PM  
Deleted: 7

Amy Solomon 7/28/2015 10:01 PM  
Deleted: ure  
Amy Solomon 7/28/2015 10:01 PM  
Deleted: 7

947 below (Fig. 9b). Due to the additional activation of IN as the cloud layer cools, ice  
948 production is maintained in the absence of recycling and the activation of IN in the cloud  
949 layer exceeds the upward IN flux at cloud base (Fig. 9a,b). However, the diminishing  $N_{IN}$  in  
950 the subcloud layer limits IN activation and  $N_{ICE}$  rapidly decreases in the cloud layer (Fig. 8d).

### 951 4.3 Impact of diurnal cycle

952 A diurnal cycle is added to the Control simulation in order to investigate how the feedback  
953 loops identified in the Control and NoRecycle runs are modified with realistic transient  
954 heating and cooling tendencies due to variations in incoming shortwave radiation. A question  
955 that is addressed in this diurnal simulation is, to what extent is the continuous production of  
956 ice in the Control simulation due to the lack of incoming shortwave radiation, which may  
957 overestimate the cooling tendencies in the cloud layer, resulting in an overestimate of IN  
958 activation? In addition, we investigate whether allowing for a realistic diurnal cycle provides  
959 for additional buffering feedbacks.

960 Adding a diurnal cycle to the Control simulation produces a diurnal peak in downwelling  
961 surface shortwave radiation of  $510 \text{ W m}^{-2}$  and 6 hours of total darkness per day (Fig. 11b).  
962 As shortwave radiation increases, the net radiative cooling near cloud top diminishes, which  
963 decreases cloud-generated turbulence, decreasing LWP and cloud-layer thickness. In addition,  
964 it is seen that the peak daily LWP coincides with zero shortwave radiation when in-cloud  
965 turbulence and cloud thickness are largest (Fig. 11a). These values are on the low end but  
966 within the measurements for this ISDAC case.

Amy Solomon 7/28/2015 10:01 PM  
Deleted: ure

Amy Solomon 7/28/2015 10:01 PM  
Deleted: 8

Amy Solomon 7/28/2015 10:01 PM  
Deleted: ure

Amy Solomon 7/28/2015 10:01 PM  
Deleted: 8

Amy Solomon 7/29/2015 6:04 PM  
Deleted: N

Amy Solomon 7/28/2015 10:01 PM  
Deleted: ure

Amy Solomon 7/28/2015 10:01 PM  
Deleted: 7

Amy Solomon 7/28/2015 10:01 PM  
Deleted: ure

Amy Solomon 7/28/2015 10:01 PM  
Deleted: 0

Amy Solomon 7/28/2015 10:01 PM  
Deleted: ure

Amy Solomon 7/28/2015 10:00 PM  
Deleted: 0

978 Fig. 11a,b shows that LWP and IWP variability is predominantly driven by the diurnal cycle.  
 979 However, IWP variability is seen to lag LWP by 3-4 hours because as shortwave radiation  
 980 decreases the cloud layer cools, which increases activation of IN, increasing  $N_{ICE}$ , allowing  
 981 more ice crystals to grow, which increases IWP (Fig. 11a,b). Similar to the Control  
 982 simulation subcloud  $N_{IN}$  decreases at a faster rate than cloud layer  $N_{ICE}$ , but allowing for the  
 983 warming and cooling tendencies in the diurnal cycle results in cloud layer  $N_{ICE}$  that decreases  
 984 40% more slowly than in the Control simulation (Fig. 11c).

985 Precipitation and turbulent mixing of  $N_{ICE}$  (hereafter turbulent mixing is referred to as  
 986 “ $T_{ICE}$ ”) at cloud base are out of phase by 10 hours (Fig. 11d), with turbulence leading  
 987 precipitation. When shortwave radiation is weak or absent, the increase in  $N_{ICE}$  eventually  
 988 becomes limited by a decreasing turbulent mixing of IN (“ $T_{IN}$ ”) into the cloud layer from  
 989 below, as recycling slows due to a decrease in  $N_{ICE}$  flux from the cloud layer (Fig. 11d,f).  
 990 When shortwave radiation is strong, reduction in IWP is limited by weaker precipitation  
 991 losses, and attendant weaker sublimation and IN flux into the cloud layer (Fig. 11d,f).  
 992 Entrainment of  $N_{IN}$  at the mixed-layer top is insignificant throughout the integration (Fig.  
 993 11e).

994 **5 Analysis from a mixed-layer perspective**

995 The results discussed in Section 4 can be understood from balances in a well-mixed layer  
 996 with sources/sinks at the upper and lower boundaries. Total particle concentration  
 997 ( $N_{IN}+N_{ICE}$ ) is only changed by fluxes at the mixed-layer boundaries when recycling is  
 998 allowed. These fluxes are entrainment of  $N_{IN}$  at mixed-layer top and turbulent mixing of both

Amy Solomon 7/28/2015 10:00 PM  
 Deleted: ures

Amy Solomon 7/28/2015 10:00 PM  
 Deleted: 1

Amy Solomon 7/28/2015 10:00 PM  
 Deleted: 0

Amy Solomon 7/29/2015 6:04 PM  
 Deleted: N

Amy Solomon 7/28/2015 10:00 PM  
 Deleted: ure

Amy Solomon 7/28/2015 10:00 PM  
 Deleted: 0

Amy Solomon 7/29/2015 6:04 PM  
 Deleted: N

Amy Solomon 7/29/2015 6:05 PM  
 Deleted: N

Amy Solomon 7/28/2015 10:00 PM  
 Deleted: ure

Amy Solomon 7/28/2015 10:00 PM  
 Deleted: 0

Amy Solomon 7/29/2015 6:05 PM  
 Deleted: N

Amy Solomon 7/29/2015 6:05 PM  
 Deleted: N

Amy Solomon 7/28/2015 10:00 PM  
 Deleted: ure

Amy Solomon 7/28/2015 10:00 PM  
 Deleted: 0

Amy Solomon 7/29/2015 6:05 PM  
 Deleted: N

Amy Solomon 7/29/2015 6:05 PM  
 Deleted: N

Amy Solomon 7/28/2015 9:59 PM  
 Deleted: ure

Amy Solomon 7/28/2015 9:59 PM  
 Deleted: 0

Amy Solomon 7/28/2015 10:00 PM  
 Deleted: ure

Amy Solomon 7/28/2015 9:59 PM  
 Deleted: 0

Amy Solomon 7/28/2015 10:00 PM  
 Deleted: ure

Amy Solomon 7/28/2015 9:59 PM  
 Deleted: 0

Amy Solomon 7/29/2015 6:06 PM  
 Deleted: N

1022  $N_{ICE}$  and  $N_{IN}$  ( $T_{ICE}$  and  $T_{IN}$ ) and precipitation of  $N_{ICE}$  ( $P$ ) at mixed-layer base. Since there  
 1023 are no sources and sinks of  $N_{IN}+N_{ICE}$  within the mixed layer, the horizontally-averaged  
 1024  $N_{IN}+N_{ICE}$  flux ( $f(z)$ ) must vary linearly from mixed-layer base to mixed-layer top (Lilly,  
 1025 1968; Bretherton and Wyant, 1997). If it is assumed that  $f$  at the mixed-layer base is  
 1026 downward (assumed negative in this formulation) and  $f$  at the mixed-layer top is negligible  
 1027 (robust assumptions for a scenario where ice is precipitating from the mixed layer and  
 1028 entrainment is weak), then

$$f(z) = R * \frac{H - z}{H - B}, \quad B \leq z \leq H \quad (5)$$

1029 where  $H$  is the mixed-layer height,  $B$  is the mixed-layer base and  $R$  is the total  $N_{IN}+N_{ICE}$  flux  
 1030 at the mixed-layer base,

$$R = f|_{\text{Mixed-Layer Base}} = [P + T_{ICE} + T_{IN}]_{\text{Mixed-Layer Base}}, \quad (6)$$

1031 and

$$[T_{ICE} + T_{IN}]_{\text{Cloud Base}} \approx [f - P]_{\text{Cloud Base}}. \quad (7)$$

1032 Since  $f < 0$ , the turbulent flux of  $N_{IN}$  into the cloud layer plus the turbulent flux of  $N_{ICE}$  into  
 1033 the subcloud layer is always less than precipitation of  $N_{ICE}$  at cloud base. In addition, in a  
 1034 slowly evolving state where  $T_{IN}|_{\text{Mixed-Layer Base}} > 0$ , total IN flux due to sublimation in the  
 1035 mixed layer,  $S$ , can be written as

Amy Solomon 7/29/2015 6:06 PM  
 Deleted: N  
 Amy Solomon 7/29/2015 6:06 PM  
 Deleted: N  
 Amy Solomon 7/29/2015 6:06 PM  
 Deleted: N  
 Amy Solomon 7/29/2015 6:06 PM  
 Deleted: N  
 Amy Solomon 7/29/2015 6:06 PM  
 Deleted: N

Amy Solomon 7/29/2015 6:06 PM  
 Deleted: N

Amy Solomon 7/29/2015 6:06 PM  
 Deleted: N

Amy Solomon 7/29/2015 6:06 PM  
 Deleted: N

Amy Solomon 7/29/2015 6:07 PM  
 Deleted: N

Amy Solomon 7/29/2015 6:07 PM  
 Deleted: N

$$S \approx [P + T_{ICE}]_{\text{Mixed-Layer Base}} - [P + T_{ICE}]_{\text{Cloud Base}} \quad (8a)$$

1046  $\approx [f - T_{IN}]_{\text{Mixed-Layer Base}} - [f - T_{IN}]_{\text{Cloud Base}} \quad (8b)$

1047 and since  $f|_{\text{Mixed-Layer Base}}$  is downward and  $f|_{\text{Mixed-Layer Top}}$  is negligible (eq. 5),

$$S < T_{IN}|_{\text{Cloud Base}} - T_{IN}|_{\text{Mixed-Layer Base}} \quad (8c)$$

$$< T_{IN}|_{\text{Cloud Base}} \cdot \quad (8d)$$

1048 Thus in a well-mixed layer with an upward  $T_{IN}|_{\text{Mixed-Layer Base}}$  sublimation is always less than  
1049 the flux of  $N_{IN}$  into the cloud layer.

1050 Based on results from Control, precipitation of  $N_{ICE}$  at cloud base is sufficient to balance the  
1051 upward turbulent flux of  $N_{IN}$  (i.e.,  $|T_{IN}| \gg |T_{ICE}|$  at cloud base). Therefore, in a well-mixed  
1052 layer with precipitation of  $N_{ICE}$  at the mixed-layer base that is larger in magnitude than an  
1053 upward turbulent  $N_{IN}$  flux at the mixed-layer base, and assuming negligible entrainment at  
1054 the mixed-layer top

$$|P|_{\text{Cloud Base}} > T_{IN}|_{\text{Cloud Base}} > S. \quad (9)$$

1055 However, if all  $N_{ICE}$  sublimate in the mixed layer and the upward turbulent flux of  $N_{IN}$   
1056 dominates at the mixed-layer base then  $f > 0$  and

$$T_{IN}|_{\text{Cloud Base}} > |P|_{\text{Cloud Base}} = S, \quad (10)$$

Amy Solomon 7/29/2015 6:07 PM

Deleted: N

Amy Solomon 7/29/2015 6:07 PM

Deleted: N

Amy Solomon 7/29/2015 5:31 PM

Deleted:

Amy Solomon 7/29/2015 5:31 PM

Deleted:

Amy Solomon 7/29/2015 6:07 PM

Deleted: N

Amy Solomon 7/29/2015 6:07 PM

Deleted: N

Amy Solomon 7/29/2015 6:07 PM

Deleted: N

Amy Solomon 7/29/2015 6:08 PM

Deleted: N

1065 the mixed layer gains  $N_{IN} + N_{ICE}$  over time, resulting in a continuously increasing ice  
1066 production in the cloud layer. In the presence of shortwave radiation (i.e., in the SW  
1067 simulation),  $T_{IN}|_{Cloud\ Base}$  is also greater than  $|P|_{Cloud\ Base}$  after a period of weakened  
1068 turbulence and weaker precipitation at the mixed-layer base, due to increased activation of  
1069  $N_{IN}$  due to decreasing shortwave radiation.

Amy Solomon 7/29/2015 6:08 PM  
Deleted: N

Amy Solomon 7/29/2015 4:50 PM  
Deleted: SW

1070 If IN entrainment at the mixed-layer top is not negligible then  $f(z)$  must be modified to  
1071 include fluxes at the mixed-layer top and  $|f|_{Cloud\ Base}$  will increase. If  $|f|_{Cloud\ Base}$  increases  
1072 such that  $f_{Cloud\ Base} < P_{Mixed-Layer\ Base}$ , then sublimation will exceed  $T_{IN}|_{Cloud\ Base}$ .

1073 This mixed-layer analysis provides a framework to understand the results presented in  
1074 Section 4. Specifically, sublimation being less than the turbulent flux of IN is seen to be a  
1075 property of a well-mixed layer where the total flux at mixed-layer base is downward and the  
1076 total flux at the mixed-layer top is negligible. In the case where the mixed layer is saturated  
1077 with respect to ice, sublimation is equal to zero and the turbulent flux of IN at the mixed-  
1078 layer base is less than the turbulent flux of IN at the cloud base, reducing the flux of IN into  
1079 the cloud layer. The relationships outlined in this section are appropriate for any AMPS with  
1080 weak entrainment at cloud top, weak large-scale advective fluxes, and net downward fluxes  
1081 at the mixed-layer base.

## 1082 **6 Analysis of Buffered Feedbacks in SW**

1083 Phase diagrams highlight the processes involved in ice production when a diurnal cycle is  
1084 allowed (following the arrows from green to blue to black to red in Fig. 12a,b). When  
1085 incoming shortwave radiation is a maximum, recycling (sublimation) is seen to be at a

Amy Solomon 7/28/2015 9:59 PM  
Deleted: ures

Amy Solomon 7/28/2015 9:59 PM  
Deleted: 1

1090 minimum. This is counterintuitive since subcloud relative humidity is low at this time, which  
 1091 would be expected to produce increased sublimation. However, due to weak turbulent mixing  
 1092 between the cloud and subcloud layers the net  $N_{ICE}$  flux into the subcloud layer is weak,  
 1093 resulting in weak sublimation and recycling. This situation is reversed as shortwave radiation  
 1094 decreases, since increased cloud-top cooling increases cloud-driven turbulent mixing, which  
 1095 allows recycling to increase in the regions of reduced subcloud relative humidity. As is seen  
 1096 in the conceptual diagram (Fig. 10), this then leads to an increased  $N_{ICE}$  flux into the  
 1097 subcloud layer (green arrows, Fig. 12). However,  $N_{ICE}$  in the cloud layer doesn't begin to  
 1098 increase until activation in the cloud layer exceeds the flux of  $N_{ICE}$  into the subcloud layer  
 1099 (green arrows). This cycle is further amplified as shortwave radiation decreases, namely,  
 1100 decreased shortwave radiation increases cloud-driven turbulence, increasing the flux of IN  
 1101 into the cloud layer, increasing the activation of IN, which increases  $N_{ICE}$  in the cloud layer  
 1102 and the  $N_{ICE}$  flux from the cloud layer into the subcloud layer (blue arrows).

1103 When incoming shortwave radiation is a minimum, more  $N_{IN}$  are activated because the cloud  
 1104 layer cools. However, again we see that  $N_{ICE}$  tendencies due to thermodynamics are buffered  
 1105 by the slowing of turbulence-driven feedbacks due to a thickening of the cloud layer. Thus, a  
 1106 net increase in  $N_{ICE}$  in the cloud layer, commensurate with an increased IWP and  
 1107 precipitation (black arrows), is buffered by a decrease in the downward turbulent mixing of  
 1108  $N_{ICE}$ , which reduces recycling, slowing the feedback loop (see Fig. 10). During the morning  
 1109 hours, as the cloud layer warms and thins and ice activation becomes less efficient,  
 1110 turbulence continues to decline, slowing the recycling feedback process to the point where  
 1111 limited IN fluxes to the cloud layer inhibit ice production and  $N_{ICE}$  declines (red arrows).

Amy Solomon 7/29/2015 6:08 PM  
 Deleted: N

Amy Solomon 7/28/2015 9:58 PM  
 Deleted: ure

Amy Solomon 7/28/2015 9:58 PM  
 Deleted: 9

Amy Solomon 7/29/2015 6:08 PM  
 Deleted: N

Amy Solomon 7/28/2015 9:58 PM  
 Deleted: 1

Amy Solomon 7/29/2015 6:09 PM  
 Deleted: N

Amy Solomon 7/29/2015 6:09 PM  
 Deleted: N

Amy Solomon 7/29/2015 6:09 PM  
 Deleted: N

Amy Solomon 7/29/2015 6:09 PM  
 Deleted: N

Amy Solomon 7/29/2015 5:36 PM  
 Deleted:  $N_{IN}$

Amy Solomon 7/29/2015 6:09 PM  
 Deleted: N

Amy Solomon 7/29/2015 6:09 PM  
 Deleted: N

Amy Solomon 7/29/2015 6:09 PM  
 Deleted: N

Amy Solomon 7/29/2015 6:09 PM  
 Deleted: N

Amy Solomon 7/29/2015 6:09 PM  
 Deleted: N

Amy Solomon 7/28/2015 9:59 PM  
 Deleted: ure

Amy Solomon 7/28/2015 9:58 PM  
 Deleted: 9

Amy Solomon 7/29/2015 6:09 PM  
 Deleted: N

1128 **7 Summary**

1129 We have demonstrated that sustained recycling of IN through a drying subcloud layer and  
1130 additional activation of  $N_{IN}$  due to a cooling cloud layer are sufficient to maintain ice  
1131 production, and regulate liquid production over multiple days in a decoupled AMPS.

1132 This study provides an idealized framework to understand feedbacks between dynamics and  
1133 microphysics that maintain phase-partitioning in AMPS. In addition, we have shown that  
1134 modulation of the cooling of the cloud layer and the humidity of the subcloud layer by the  
1135 diurnal cycle buffers the mixed-layer system from a loss of particles and promotes the  
1136 persistence of a mixed-phase cloud system. The results of this study provide insight into the  
1137 mechanisms and feedbacks that may maintain cloud ice in AMPS even when entrainment of  
1138 IN at the mixed-layer boundaries is weak. While the balance of these processes changes  
1139 depending upon the specific conditions of the cloud layer, for example whether the  
1140 cloud layer is coupled to the surface layer, the mechanisms detailed in this paper will  
1141 manifest to some degree and therefore the current study provides a framework for  
1142 understanding the role of recycling in maintaining phase-partitioning in AMPS.



1143 **Author Contributions:**

1144 A.S., G.F., and M.D.S. conceived and designed the experiments; A.S. performed the  
1145 simulations; A.S., G.F., and M.D.S. analyzed the model results and co-wrote the paper.

1146 **Acknowledgements:**

1147 The authors acknowledge discussions with Alex Avramov, Chris Cox, Gijs de Boer, Barbara  
1148 Ervens, and Ann Fridlind, and Takanobu Yamaguchi for developing the software to run  
1149 WRF as a large eddy simulation. This research was supported by the Office of Science  
1150 (BER), U.S. Department of Energy (DE-SC0011918) and the National Science Foundation  
1151 (ARC-1023366).

1152 **References**

- 1153 Abdul-Razzak, H. and Ghan, S. J.: A parameterization of aerosol activation 2. Multiple  
1154 aerosol types, *J. Geophys. Res.*, 105, 683–6844, 2000.
- 1155 Avramov, A., Ackerman, A. S., Fridlind, A. M., van Dierenhoven, B., Botta, G., Aydin, K.,  
1156 Verlinde, J., Korolev, A. V., Strapp, J. W., McFarquhar, G. M., Jackson, R., Brooks, S.  
1157 D., Glen, A., and Wolde, M.: Toward ice formation closure in Arctic mixed-phase  
1158 boundary layer clouds during ISDAC, *J. Geophys. Res.*, 116, D00T08,  
1159 doi:10.1029/2011JD015910, 2011.
- 1160 Barton, N. P., Klein, S. A., Boyle, J. S., and Zhang, Y. Y.: Arctic synoptic regimes:  
1161 Comparing domain wide Arctic cloud observations with CAM4 and CAM5 during  
1162 similar dynamics, *J. Geophys. Res.*, 117, D15205, doi:10.1029/2012JD017589, 2012.
- 1163 Bennartz, R., Shupe, M., Turner, D., Walden, V., Steffen, K., Cox, C., Kulie, M. S., Miller,  
1164 N., and Pettersen, C.: July 2012 Greenland melt extent enhanced by low-level liquid  
1165 clouds, *Nature*, 496, 83-86, doi:10.1038/nature12002, 2012.
- 1166 Birch, C. E., Brooks, I. M., Tjernström, M., Shupe, M. D., Mauritsen, T., Sedlar, J., Lock, A.  
1167 P., Earnshaw, P., Persson, P. O. G., Milton, S. F., and Leck, C.: Modeling atmospheric  
1168 structure, cloud and their response to CCN in the central Arctic: ASCOS case studies,  
1169 *Atmos. Chem. Phys.*, 12, 3419-3435, doi:10.5194/acp-12-3419-2012, 2012.
- 1170 Bretherton, C. S. and Wyant, M. C.: Moisture transport, lower-tropospheric stability, and  
1171 decoupling of cloud-topped boundary layers, *J. Atmos. Sci.*, 54, 148-167, 1997.
- 1172 Broadley, S., Murray, B., Herbert, R., Atkinson, J., Dobbie, S., Malkin, T., Condliffe, E., and  
1173 Neve, L.: Immersion mode heterogeneous ice nucleation by an illite rich powder  
1174 representative of atmospheric mineral dust, *Atmos. Chem. Phys.*, 12:287{307,

Amy Solomon NOAA 7/30/2015 2:32 PM  
Deleted: 6837

1176 doi:10.5194/acp-12-287-2012, 2012.

1177 Chen, J.-P. and Lamb, D.: The theoretical basis for the parameterization of ice crystal habits:  
1178 Growth by vapor deposition, *J. Atmos. Sci.*, 51, 1206–1222, doi:10.1175/1520-  
1179 0469(1994)051<1206:TTBFTP>2.0.CO;2, 1994.

1180 Collins, W. D., Rasch, P. J., Boville, B. A., Hack, J. J., McCaa, J. R., Williamson, D. L., and  
1181 Briegleb, B. P.: Description of the NCAR Community Atmosphere Model (CAM 3.0),  
1182 NCAR Technical Note, NCAR/TN-464+STR, 226 pp., 2004.

1183 Curry, J. and Ebert, E. E.: Annual cycle of radiation fluxes over the Arctic Ocean: Sensitivity  
1184 to cloud optical properties, *J. Climate*, 5, 1267–1280, 1992.

1185 Cziczo, D., Froyd, K., Gallavardin, S., Moehler, O., Benz, S., Saatho, H., and Murphy, D.:  
1186 Deactivation of ice nuclei due to atmospherically relevant surface coatings, *Environ.*  
1187 *Res. Lett.*, 4:044013, doi:10.1088/1748-9326/4/4/044013, 2009.

1188 de Boer, G., Chapman, W., Kay, J. E., Medeiros, B., Shupe, M. D., Vavrus, S., and Walsh, J.:  
1189 A characterization of the present-day Arctic atmosphere in CCSM4, *J. Climate*, 25,  
1190 2676–2695, 2012.

1191 DeMott, P. J.: An exploratory study of ice nucleation by soot aerosols, *J. Appl. Meteorol.*,  
1192 29(10), 1072–1079, 1990.

1193 DeMott, P. J., Prenni, A. J., Liu, X., Petters, M. D., Twohy, C. H., Richardson, M. S.,  
1194 Eidhammer, T., Kreidenweis, S. M., and Rogers, D. C.: Predicting global atmospheric  
1195 ice nuclei distributions and their impacts on climate, *P. Natl. Acad. Sci. USA*, 107,  
1196 11217–11222, doi:10.1073/pnas.0910818107, 2010.

1197 Dyer, A. J. and Hicks, B. B.: Flux-gradient relationships in the constant flux layer, *Q. J. Roy.*  
1198 *Meteor. Soc.*, 96, 715–721, 1970.

Amy Solomon NOAA 7/30/2015 2:32 PM  
Deleted: \_

1200 Ervens, B., Feingold, G., Sulia, K., and Harrington, J.: The impact of microphysical  
1201 parameters, ice nucleation mode, and habit growth on the ice/liquid partitioning in  
1202 mixed-phase Arctic clouds, *J. Geophys. Res.*, 116, D17205,  
1203 doi:10.1029/2011JD015729, 2011.

1204 Fan, J., Ovchinnikov, M., Comstock, J. M., McFarlane, S. A., and Khain, A.: Ice formation  
1205 in Arctic mixed-phase clouds: Insights from a 3-D cloud-resolving model with size-  
1206 resolved aerosol and cloud microphysics, *J. Geophys. Res.*, 114, D04205,  
1207 doi:10.1029/2008JD010782, 2009.

1208 Feingold, G., Kreidenweis, S. M., Stevens, B., and Cotton, W. R.: Numerical simulation of  
1209 stratocumulus processing of cloud condensation nuclei through collision-coalescence, *J.*  
1210 *Geophys. Res.*, 101, 21,391-21,402, 1996.

1211 Fridlind, A. M., van Dierenhoven, B., Ackerman, A. S., Avramov, A., Mrowiec, A.,  
1212 Morrison, H., Zuidema, P., and Shupe, M. D.: A FIRE-ACE/SHEBA case study of  
1213 mixed-phase Arctic boundary-layer clouds: Entrainment rate limitations on rapid  
1214 primary ice nucleation processes, *J. Atmos. Sci.*, 69, 365-389, doi:10.1175/JAS-D-11-  
1215 052.1, 2012.

1216 Hobbs, P. V. and Rangno A. L.: Microstructure of low and middle- level clouds over the  
1217 Beaufort Sea, *Q. J. Roy. Meteor. Soc.*, 124, 2035-2071, 1998.

1218 Hoose, C. and Möhler, O.: Heterogeneous ice nucleation on atmospheric aerosols: a review  
1219 of results from laboratory experiments, *Atmos. Chem. Phys.*, 12, 9817-9854,  
1220 doi:10.5194/acp-12-9817-2012, 2012.

1221 Iacono, M. J., Delamere, J. S., Mlawer, E. J., Shephard, M. W., Clough, S. A., and Collins,  
1222 W. D.: Radiative forcing by long-lived greenhouse gases: Calculations with the AER

1223 Radiative transfer models, *J. Geophys. Res.*, 113, D13103, doi:10.1029/2008JD009944,  
1224 2008.

1225 Intrieri, J. M., Fairall, C. W., Shupe, M. D., Persson, P. O. G., Andreas, E., Guest, P. S., and  
1226 Moritz, R. E.: An annual cycle of Arctic surface cloud forcing at SHEBA, *J. Geophys.*  
1227 *Res.*, 107, 8039, doi:10.1029/2000JC000439, 2002.

1228 Kanji, Z., DeMott, P., Möhler, O., and Abbatt, J.: Results from the University of Toronto  
1229 continuous flow diffusion chamber at ICIS 2007: instrument intercomparison and ice  
1230 onsets for different aerosol types, *Atmos. Chem. Phys.*, 11:31-41, doi:10.5194/acp-11-  
1231 31-2011, 2011.

1232 Karlsson, J. and Svensson, G.: The simulation of Arctic clouds and their influence on the  
1233 winter surface temperature in present-day climate in the CMIP3 multi-model dataset,  
1234 *Clim. Dynam.*, 36, 623–635, 2011.

1235 Klein, S. A., McCoy, R., Morrison, H., Ackerman, A., Avramov, A., de Boer, G., Chen, M.,  
1236 Cole, J., DelGenio, A. D., Falk, M., Foster, M., Fridlind, A., Golaz, J.-C., Hashino, T.,  
1237 Harrington, J., Hoose, C., Khairoutdinov, M., Larson, V., Liu, X., Luo, Y., McFarquhar,  
1238 G., Menon, S., Neggers, R., Park, S., von Salzen, K., Schmidt, J. M., Sednev, I.,  
1239 Shipway, B., Shupe, M., Spangenberg, D., Sud, Y., Turner, D., Veron, D., Walker, G.,  
1240 Wang, Z., Wolf, A., Xie, S., Xu, K.-M., Yang, G., and Zhang, G.: Intercomparison of  
1241 model simulations of mixed-phase clouds observed during the ARM Mixed-Phase Arctic  
1242 Cloud Experiment. I: Single-layer cloud, *Q. J. Roy. Meteor. Soc.*, 135, 979–1002, 2009.

1243 Korolev, A.: Limitations of the Wegener–Bergeron–Findeisen mechanism in the evolution of  
1244 mixed-phase clouds, *J. Atmos. Sci.*, 64, 3372–3375, doi:10.1175/JAS4035.1, 2007.

1245 Korolev, A. and Sussman, B.: A technique for habit classification of cloud particles, *J. Atmos.*  
1246 *Oceanic Technol.*, 17, 1048–1057, 2000.

1247 Kulkarni, G., Fan, J., Comstock, J., Liu, X., and Ovchinnikov, M.: Laboratory measurements  
1248 and model sensitivity studies of dust deposition ice nucleation, *Atmos. Chem. Phys.*,  
1249 12:7295-7308, doi:10.5194/acp-12-7295-2012, 2012.

1250 Levin, Z. and Yankofsky, S.: Contact versus immersion freezing of freely suspended droplets  
1251 by bacterial ice nuclei, *J. Appl. Meteorol. Clim.*, 22, 1964-1966, 1983.

1252 Lilly, D. K.: Models of cloud-topped mixed layers under a strong inversion, *Q. J. Roy.*  
1253 *Meteor. Soc.*, 94, 292–309, 1968.

1254 Lüönd, F., Stetzer, O., Welti, A., and Lohmann, U.: Experimental study on ice nucleation  
1255 ability of size selected kaolinite particles in the immersion mode, *J. Geophys. Res.*,  
1256 115:D14201, doi:10.1029/2009JD012959, 2010.

1257 McFarquhar, G. M., Zhang, G., Poellot, M. R., Kok, G. L., McCoy, R., Tooman, T., Fridlind,  
1258 A., and Heymsfield, A. J.: Ice properties of single-layer stratocumulus during the Mixed-  
1259 Phase Arctic Cloud Experiment: 1. Observations, *J. Geophys. Res.*, 112, D24201,  
1260 doi:10.1029/2007JD008633, 2007.

1261 McFarquhar, G. M., Ghan, S., Verlinde, J., Korolev, A., Strapp, J. W., Schmid, B.,  
1262 Tomlinson, J. M., Wolde, M., Brooks, S. D., Cziczo, D., Dubey, M. K., Fan, J., Flynn,  
1263 C., Gultepe, I., Hubbe, J., Gilles, M. K., Laskin, A., Lawson, P., Leitch, W. R., Liu, P.,  
1264 Liu, X., Lubin, D., Mazzoleni, C., Macdonald, A.-M., Moffet, R. C., Morrison, H.,  
1265 Ovchinnikov, M., Shupe, M. D., Turner, D. D., Xie, S., Zelenyuk, A., Bae, K., Freer, M.,  
1266 and Glen, A.: Indirect and Semi-Direct Aerosol Campaign (ISDAC): The Impact of

1267 Arctic Aerosols on Clouds, *B. Am. Meteorol. Soc.*, 92, 183–201,  
1268 doi:10.1175/2010BAMS2935.1, 2011.

1269 Möhler, O., Büttner, S., Linke, C., Schnaiter, M., Saathoff, H., Stetzer, O., Wagner, R.,  
1270 Krämer, M., Mangold, A., Ebert, V., and Schurath, U.: Effect of sulfuric acid coating on  
1271 heterogeneous ice nucleation by soot aerosol particles, *J. Geophys. Res.*, 110:D11210,  
1272 doi: 10.1029/2004JD005169, 2005.

1273 Möhler, O., Field, P., Connolly, P., Benz, S., Saathoff, H., Schnaiter, M., Wagner, R., Cotton,  
1274 R., Krämer, M., Mangold, A., and Heymsfield, A.: Efficiency of the deposition mode ice  
1275 nucleation on mineral dust particles, *Atmos. Chem. Phys.*, 6:3007-3021,  
1276 doi:10.5194/acp-6-3007-2006, 2006.

1277 Morrison, H. and Pinto, J. O.: Mesoscale modeling of springtime Arctic mixed-phase  
1278 stratiform clouds using a new two-moment bulk microphysics scheme, *J. Atmos. Sci.*, 62,  
1279 3683-3704, 2005.

1280 Morrison, H., Thompson, G., and Tatarskii, V.: Impact of cloud microphysics on the  
1281 development of trailing stratiform precipitation in a simulated squall line: Comparison of  
1282 one- and two-moment schemes, *Mon. Wea. Rev.*, 137, 991-1007,  
1283 doi:10.1175/2008MWR2556.1, 2009.

1284 Paulson, C. A.: The mathematical representation of wind speed and temperature profiles in  
1285 the unstable atmospheric surface layer, *J. Appl. Meteor.*, 9, 857–861, 1970.

1286 Persson, P. O. G.: Onset and end of the summer melt season over sea ice: Thermal structure  
1287 and surface energy perspective from SHEBA, *Clim. Dynam.*, 39, 1349-1371,  
1288 doi:10.1007/s00382-011-1196-9, 2012.

1289 Pinti, V., Marcolli, C., Zobrist, B., Hoyle, C., and Peter, T.: Ice nucleation efficiency of clay  
1290 minerals in the immersion mode, *Atmos. Chem. Phys.*, 12:5859-5878, doi:10.5194/acp-  
1291 12-5859-2012, 2012.

1292 Pruppacher, H. and Klett, J.: *Microphysics of clouds and precipitation*. Kluwer Academic  
1293 Publishers, 2nd edition, 1997.

1294 Roberts, P. and Hallett, J.: A laboratory study of the ice nucleating properties of some  
1295 mineral particulates, *Q. J. R. Meteorol. Soc.*, 94, 25 – 34, 1967.

1296 Sandvik, A., Biryulina, M., Kvamsto, N., Stamnes, J., and Stamnes, K.: Observed and  
1297 simulated microphysical composition of Arctic clouds: Data properties and model  
1298 validation, *J. Geophys. Res.* 112, D05205, 2007.

1299 Sedlar, J., Shupe, M. D., and Tjernström, M.: On the relationship between thermodynamic  
1300 structure, cloud top, and climate significance in the Arctic, *J. Climate*, 25, 2374–2393,  
1301 2012.

1302 Sedlar, J., Tjernström, M., Mauritsen, T., Shupe, M. D., Brooks, I. M., Persson, P. O. G.,  
1303 Birch, C. E., and C. Leck, C.: A transitioning Arctic surface energy budget: The impacts  
1304 of solar zenith angle, surface albedo and cloud radiative forcing, *Clim. Dynam.*, 37,  
1305 1643–1660, doi:10.1007/s00382-010-0937-5, 2011.

1306 Serreze, M. C., Barrett, A. P., and Stroeve, J.: Recent changes in tropospheric water vapor  
1307 over the Arctic as assessed from radiosondes and atmospheric reanalyses. *J. Geophys.*  
1308 *Res.*, 117, D10104, doi:10.1029/2011JD017421, 2012.

1309 Sheridan, L. M., Harrington, J. Y., Lamb, D., and Sulia, K.: Influence of ice crystal aspect  
1310 ratio on the evolution of ice size spectra during vapor depositional growth, *J. Atmos. Sci.*,  
1311 66, 3732–3743, doi:10.1175/2009JAS3113.1, 2009.



1312 Shupe, M. D.: A ground-based multiple remote-sensor cloud phase classifier, *Geophys. Res.*  
1313 *Lett.*, 34, L2209, doi:10.1029/2007GL031008, 2007.

1314 Shupe, M. D and J. M. Intrieri: Cloud radiative forcing of the Arctic surface: The influence  
1315 of cloud properties, surface albedo, and solar zenith angle, *J. Climate*, 17, 616-628, 2004.

1316 Shupe, M. D, Matrosov, S. Y., and Uttal, T.: Arctic mixed phase cloud properties derived  
1317 from surface-based sensors at SHEBA, *J. Atmos. Sci.*, 63, 697-811, 2006.

1318 Shupe, M. D, Persson, P. O. G., Brooks, I. M., Tjernström, M., Sedlar, J., Mauritsen, T.,  
1319 Sjogren, S., and Leck, C.: Cloud and boundary layer interactions over the Arctic sea-ice  
1320 in late summer, *Atmos. Chem. Phys.*, 13, 9379-9400, 2013.

1321 Skamarock, W. C., Klemp, J. B., Dudhia, J., Gill, D. O., Barker, D. M., Duda, M. G., Huang,  
1322 X.-Y., Wang, W., and Powers, J. G.: A description of the Advanced Research WRF  
1323 version 3, NCAR Tech. Note NCAR/TN-475+STR, 113 pp., 2008.

1324 Solomon, A., Morrison, H., Persson, P. O. G., Shupe, M. D., and Bao, J.-W.: Investigation of  
1325 microphysical parameterizations of snow and ice in Arctic clouds during M-PACE  
1326 through model-observation comparisons, *Mon. Wea. Rev.*, 137, 3110-3128,  
1327 doi:10.1175/2009MWR2688.1, 2009.

1328 Solomon, A., Shupe, M. D., Persson, P. O. G., and Morrison, H.: Moisture and dynamical  
1329 interactions maintaining decoupled Arctic mixed-phase stratocumulus in the presence of  
1330 a humidity inversion, *Atmos. Chem. Phys.*, 11, 10127-10148, doi:10.5194/acp-11-10127-  
1331 2011, 2011.

1332 Solomon, A., Shupe, M. D., Persson, P. O. G., Morrison, H., Yamaguchi, T., Caldwell, P. M.,  
1333 and de Boer, G.: The sensitivity of springtime Arctic mixed-phase stratocumulus clouds

1334 to surface layer and cloud-top inversion layer moisture sources, *J. Atmos. Sci.*, 71, 574-  
1335 595, doi:10.1175/JAS-D-13-0179.1, 2014.

1336 Tjernström, M., Sedlar, J., and Shupe, M. D.: How well do regional climate models  
1337 reproduce radiation and clouds in the Arctic? An evaluation of ARCMIP simulations, *J.*  
1338 *Appl. Met. Clim.*, 47, 2405–2422, 2008.

1339 Tjernström, M., C. Leck, C., Persson, P. O. G., Jensen, M. L., Oncley, S. P., and Targino, A.:  
1340 The summertime Arctic atmosphere: Meteorological measurements during the Arctic  
1341 Ocean Experiment 2001, *B. Am. Meteorol. Soc.*, 85, 1305–1321, 2004.

1342 Turner, D. D., Clough, S. A., Liljegren, J. C., Clothiaux, E. E., Cady-Pereira, K., and Gaustad,  
1343 K. L.: Retrieving precipitable water vapor and liquid water path from Atmospheric  
1344 Radiation Measurement (ARM) program’s microwave radiometers, *IEEE T. Geosci.*  
1345 *Remote*, 45, 3680–3690, 2007.

1346 Verlinde, J., Harrington, J. Y., McFarquhar, G. M., et al.: The Mixed-Phase Arctic Cloud  
1347 Experiment (M-PACE), *B. Am. Meteorol. Soc.*, 88, 205–221, doi:10.1175/BAMS-88-2-  
1348 205, 2007.

1349 Walsh, J. E. and Chapman, W. L.: Arctic cloud-radiation temperature associations in  
1350 observational data and atmospheric reanalyses, *J. Climate*, 11, 3030–3045, 1998.

1351 [Webb, E. K.: Profile relationships: The log-linear range, and extension to strong stability.](#)  
1352 [Quart. J. Roy. Meteor. Soc., 96, 67–90, 1970.](#)

1353 Wise, M., Baustian, K., Koop, T., Freedman, M., Jensen, E., and Tolbert, M.: Depositional  
1354 ice nucleation onto crystalline hydrated nacl particles: a new mechanism for ice  
1355 formation in the troposphere, *Atmos. Chem. Phys.*, 12:1121-1134, doi:10.5194/acp-12-  
1356 1121-2012, 2012.

1357 Yamaguchi, T. and Feingold, G.: Technical note: Large-eddy simulation of cloudy boundary  
1358 layer with the Advanced Research WRF model, *J. Adv. Model. Earth Syst.*, 4, M09003,  
1359 doi:10.1029/2012MS000164, 2012.

1360 **Figure Captions**

1361 **Figure 1:** Sounding measured at 17:34 UTC 8 April 2008 at Barrow, Alaska (71.338N,  
1362 156.68W). Left) Water vapor mixing ratio ( $q_v$ ), temperature (T), and potential temperature  
1363 (Theta), in units of  $\text{g kg}^{-1}$ , degrees Kelvin, and degrees Kelvin respectively. Right) Zonal  
1364 wind (U) and meridional wind (V), in units of  $\text{m s}^{-1}$ . Gray shading marks the extent of the  
1365 cloud layer. The dashed lines show the initial profiles used in the WRFLES experiments. The  
1366 dashed line overlaying water vapor mixing ratio is the initial profile for the total water  
1367 mixing ratio.

1368 **Figure 2:** IN number concentration active at water saturation vs. temperature based on the  
1369 empirical relationship derived in DeMott et al. (2010) (blue line) [used to initialize IN number](#)  
1370 [concentration in each bin](#). Black vertical lines indicate threshold temperatures for nucleation  
1371 in the 16 IN bins. IN increments between lines indicate the additional IN available for  
1372 nucleation at colder temperatures.

1373 **Figure 3:** Sensitivity of ice water path to the parameter F in equation (2). Note the similar ice  
1374 water paths for F=4 and F=6 (total  $N_{IN}$  initial values 5.8 and  $8.7 \text{ L}^{-1}$ , respectively).

1375 **Figure 4:** [A,B,D\) Sensitivity of LWP and IWP to snow density and fall speeds. LWP shown](#)  
1376 [with solid lines and IWP shown with dashed lines, in units of  \$\text{g m}^{-2}\$ . C\) Fall speeds used in](#)  
1377 [sensitivity studies, in units of  \$\text{m s}^{-1}\$ . A\) Sensitivity to reducing snow density from  \$100 \text{ kg m}^{-3}\$](#)   
1378 [to  \$50 \text{ kg m}^{-3}\$  \(red lines\) using Control \(CNT\) fall speeds \(red line in C\). B\) Sensitivity to](#)  
1379 [reducing snow fall speeds \(green line in C\) using Control snow density \(red lines\). D\)](#)  
1380 [Sensitivity to increasing snow fall speeds \(blue line in C\) using Control snow density \(red](#)  
1381 [lines\).](#)

Amy Solomon 7/28/2015 10:14 PM  
Formatted: Space After: 12 pt

1382 **Figure 5:** Simulated ice particle number size distributions using in-cloud mass and number  
1383 concentrations. Ice water mixing ratio =  $3e-4$  g/kg, ice number concentration =  $0.4/L$ , snow  
1384 water mixing ratio =  $2.4e-2$  g/kg, snow number concentration =  $0.45/L$ .

1385 **Figure 6:** (A)  $N_{IN}$  and (B)  $N_{ICE}$  averaged over 0.5 hours at hour 20, in units of  $L^{-1} hr^{-1}$ . Grey  
1386 shading indicates the extent of the cloud layer. Green dash lines indicate the top and bottom  
1387 of the mixed layer.

1388 **Figure 7:** Time-height cross sections of horizontally-averaged (A) IN advection plus  
1389 subsidence, in units of  $L^{-1}hour^{-1}$ , (B) ice plus snow number concentration, in units of  $L^{-1}$ , (C)  
1390 water vapor mixing ratio, in units of  $g kg^{-1}$ , and (D) relative humidity with respect to ice, in  
1391 units of percent, from CNT simulation. Temperature, in units of  $^{\circ}C$ , shown with black  
1392 contour lines in (B,C,D).

1393 **Figure 8:** Control and NoRecycle time series for hours 6-40 (smoothed with 90 minute  
1394 running average). NoRecycle shown with red and black dashed lines. A) LWP (black) and  
1395 IWP (red), in units of  $g m^{-2}$ . B) Minimum horizontally-averaged temperature in the column,  
1396 in units of  $^{\circ}C$ . C) Mixed-layer depth (blue), top height (red), and base height (black), in units  
1397 of km. D)  $N_{ICE}$  integrated over cloud layer (referred to as CL, red) and  $N_{IN}$  integrated over  
1398 subcloud layer (referred to as SubCL, black), in units of  $m L^{-1}$  (i.e., meters/liter).

1399 **Figure 9:** Horizontally-averaged fluxes from Control and NoRecycle integrations for hours  
1400 6-40 (smoothed with 90 minute running average). NoRecycle shown with red and black  
1401 dashed lines. A)  $N_{ICE}$  flux at cloud base due to turbulence+subsidence+precipitation (red),  
1402 mixed-layer base due to turbulence+subsidence+precipitation (black), and due to activation  
1403 (multiplied by -1, blue), in units of  $m L^{-1} hr^{-1}$ . B)  $N_{IN}$  flux at cloud base due to turbulence

Amy Solomon 7/29/2015 6:14 PM

Deleted: *N*

Amy Solomon 7/28/2015 10:14 PM

Formatted: Justified

Amy Solomon 7/28/2015 9:53 PM

Deleted: 7

Amy Solomon 7/28/2015 9:53 PM

Deleted: 8

Amy Solomon 7/29/2015 6:15 PM

Deleted: *N*

1408 (red),  $N_{IN}$  flux due to sublimation (black), and precipitation of  $N_{ICE}$  at cloud base (multiplied  
1409 by -1, blue), in units of  $m L^{-1} hr^{-1}$ . C)  $N_{IN}$  entrainment at mixed-layer top (red) and base  
1410 (black), in units of  $m L^{-1} hr^{-1}$ .

Amy Solomon 7/29/2015 6:15 PM  
Deleted: N

1411 **Figure 10:** Schematic of feedback loops that maintain ice production and the phase-  
1412 partitioning between cloud liquid and ice in an AMPS. Red colors denote  $N_{IN}$ . Blue colors  
1413 denote  $N_{ICE}$ . The size of the arrow indicates the relative magnitude of the flux. Vertical  
1414 profiles of  $N_{ICE}$ ,  $N_{IN}$ , relative humidity, and temperature shown with thin blue, red, green, and  
1415 yellow lines, respectively.

Amy Solomon 7/28/2015 9:54 PM  
Deleted: 9

Amy Solomon 7/29/2015 6:15 PM  
Deleted: N

Amy Solomon 7/29/2015 6:16 PM  
Deleted: N

1416 **Figure 11:** A) LWP (black) and IWP (red), in units of  $g m^{-2}$ . (B) Downward surface  
1417 shortwave radiation and turbulent kinetic energy (TKE) at cloud base, in units of  $Wm^{-2}$  and  
1418  $m^2s^{-2}$ , respectively. C)  $N_{ICE}$  in cloud layer (referred to as CL, red) and  $N_{IN}$  in subcloud layer  
1419 (referred to as SubCL, black), in units of  $m L^{-1}$ . (D) Total, turbulent, precipitation  $N_{ICE}$  flux at  
1420 cloud base (referred to as CL base, red, green, blue, respectively) and total  $N_{ICE}$  flux at  
1421 mixed-layer base (referred to as ML base, black), in units of  $m L^{-1} hr^{-1}$ , for the SW  
1422 integration for hours 16-76. Grey shading indicates hours with zero downwelling surface  
1423 shortwave radiation. E)  $N_{IN}$  entrainment at mixed-layer top (red) and base (black), in units of  
1424  $m L^{-1} hr^{-1}$ . (F)  $N_{IN}$  flux at cloud base due to turbulence (red),  $N_{IN}$  flux due to sublimation  
1425 (black), and activation of  $N_{ICE}$  (blue), in units of  $m L^{-1} hr^{-1}$ .

Amy Solomon 7/28/2015 9:54 PM  
Deleted: 0

Amy Solomon 7/29/2015 6:16 PM  
Deleted: N

Amy Solomon 7/29/2015 6:16 PM  
Deleted: N

Amy Solomon 7/29/2015 6:16 PM  
Deleted: N

1426 **Figure 12:** A) Phase diagram of TKE at cloud base vs.  $N_{ICE}$  in the cloud layer starting at  
1427 peak shortwave hour 40, in units of  $m L^{-1}$  and  $m L^{-1} hr^{-1}$ , respectively. Colors show  
1428 sublimation in units of  $m L^{-1} hr^{-1}$ . H) 24-hour phase diagrams of sublimation vs. minimum  
1429 relative humidity in the subcloud layer starting at peak shortwave hour 40, in units of  $m L^{-1}$

Amy Solomon 7/29/2015 6:16 PM  
Deleted: N

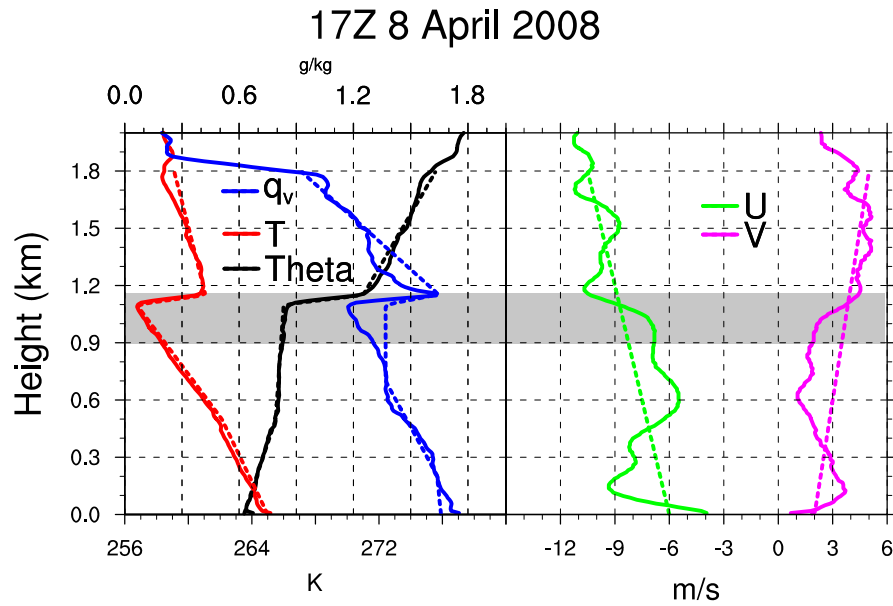
Amy Solomon 7/28/2015 9:54 PM  
Deleted: 1

Amy Solomon 7/29/2015 6:17 PM  
Deleted: NI

1441 | hr<sup>-1</sup> and %, respectively. Colors show total  $N_{CE}$  flux at cloud base, m L<sup>-1</sup> hr<sup>-1</sup>. Hours 42-47,  
1442 47-50, 50-56, and 57-62 indicated with green, blue, black, red arrows, respectively.  
1443 Minimum shortwave indicated with the moon symbol. Maximum shortwave indicated with  
1444 the sun symbol.

Amy Solomon 7/29/2015 7:13 PM

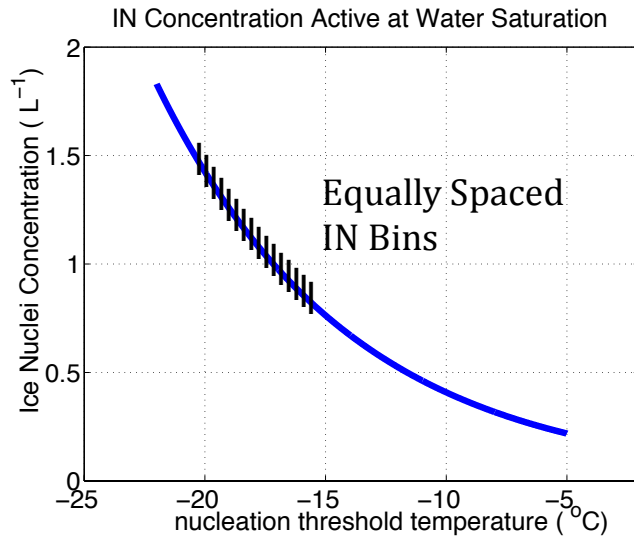
Deleted: N



1446 **Figure 1:** Sounding measured at 17:34 UTC 8 April 2008 at Barrow, Alaska (71.338N,  
 1447 156.68W). Left) Water vapor mixing ratio ( $q_v$ ), temperature ( $T$ ), and potential temperature  
 1448 ( $\Theta$ ), in units of  $\text{g kg}^{-1}$ , degrees Kelvin, and degrees Kelvin respectively. Right) Zonal  
 1449 wind ( $U$ ) and meridional wind ( $V$ ), in units of  $\text{m s}^{-1}$ . Gray shading marks the extent of the  
 1450 cloud layer. The dashed lines show the initial profiles used in the WRFLES experiments. The  
 1451 dashed line overlaying water vapor mixing ratio is the initial profile for the total water  
 1452 mixing ratio.



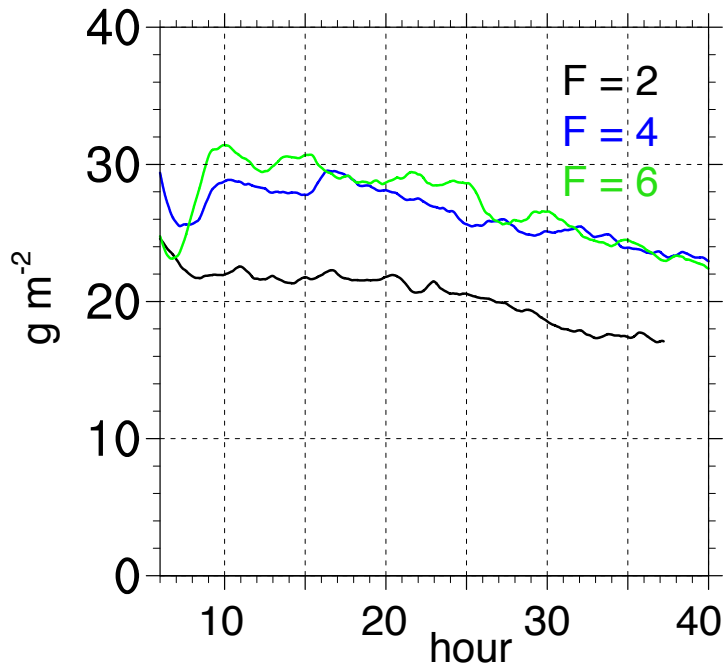
1453



1454  
1455

1456 **Figure 2:** IN number concentration active at water saturation vs. temperature based on the  
1457 empirical relationship derived in DeMott et al. (2010) (blue line) used to initialize IN number  
1458 concentration in each bin. Black vertical lines indicate threshold temperatures for nucleation  
1459 in the 16 IN bins. IN increments between lines indicate the additional IN available for  
1460 nucleation at colder temperatures.

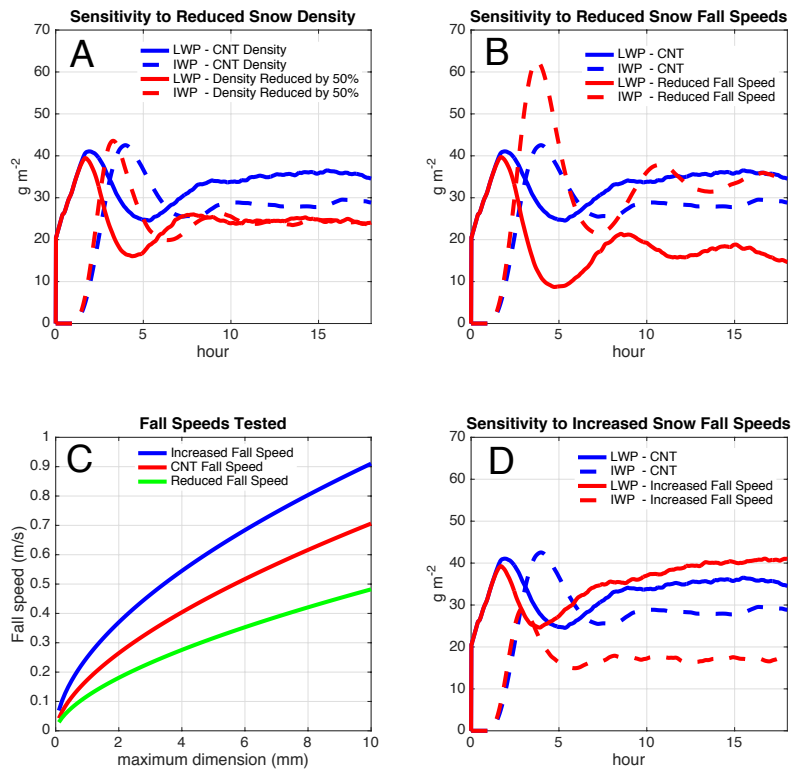
## Ice Water Paths



1461

1462 **Figure 3:** Sensitivity of ice water path to the parameter F in equation (2). Note the similar ice

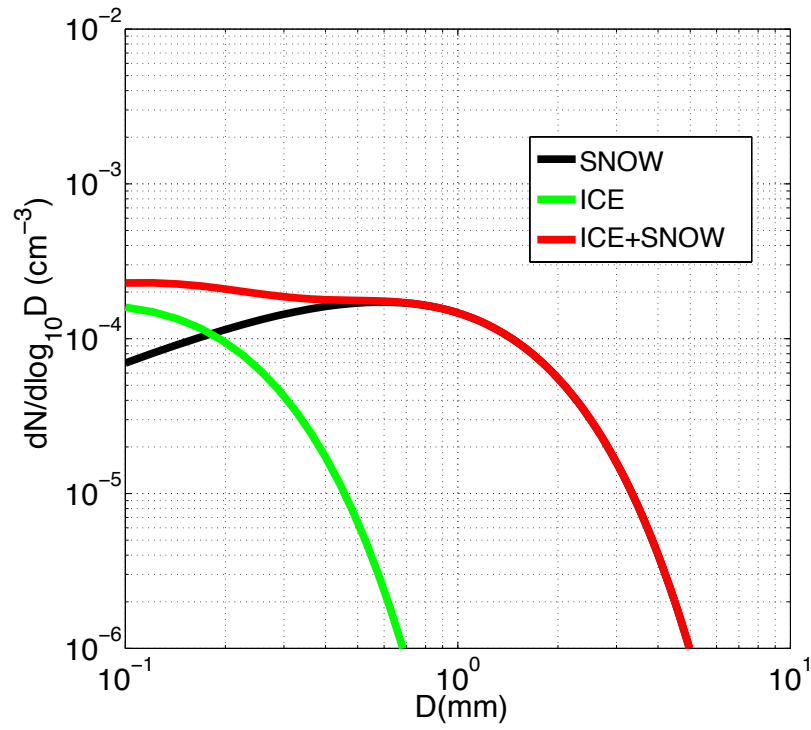
1463 water paths for F=4 and F=6 (total  $N_{IV}$  initial values of 5.8 and 8.7 L<sup>-1</sup>, respectively).



1464

1465 **Figure 4:** A,B,D Sensitivity of LWP and IWP to snow density and fall speeds. LWP shown  
 1466 with solid lines and IWP shown with dashed lines, in units of  $g\ m^{-2}$ . C Fall speeds used in  
 1467 sensitivity studies, in units of  $m\ s^{-1}$ . A) Sensitivity to reducing snow density from  $100\ kg\ m^{-3}$   
 1468 to  $50\ kg\ m^{-3}$  (red lines) using Control (CNT) fall speeds (red line in C). B) Sensitivity to  
 1469 reducing snow fall speeds (green line in C) using Control snow density (red lines). D)  
 1470 Sensitivity to increasing snow fall speeds (blue line in C) using Control snow density (red  
 1471 lines).

- Amy Solomon 7/29/2015 4:03 PM  
Formatted: Font:Not Bold
- Amy Solomon 7/29/2015 4:03 PM  
Deleted: in A,B,D
- Amy Solomon 7/29/2015 4:03 PM  
Deleted: in A,B,D
- Amy Solomon 7/29/2015 4:03 PM  
Deleted: shown in C
- Amy Solomon NOAA 7/28/2015 11:01 AM  
Deleted: compare to
- Amy Solomon NOAA 7/28/2015 11:03 AM  
Deleted: blue lines in A
- Amy Solomon NOAA 7/28/2015 11:02 AM  
Deleted: compare to blue lines in A



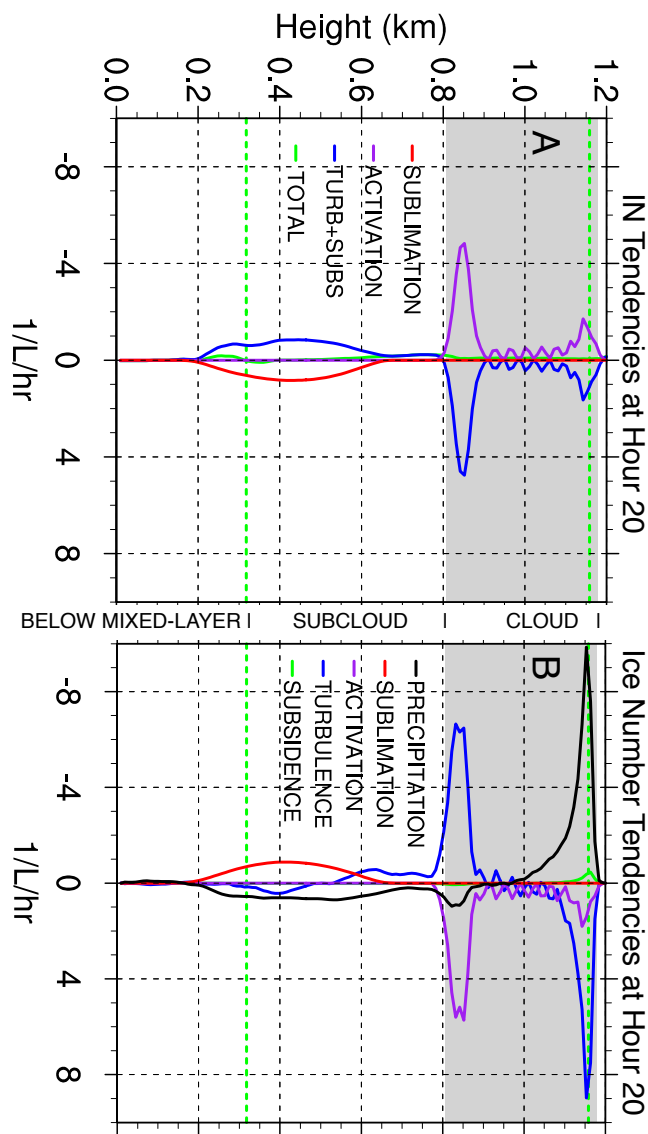
1478

1479 **Figure 5:** Simulated ice particle number size distributions using in-cloud mass and number

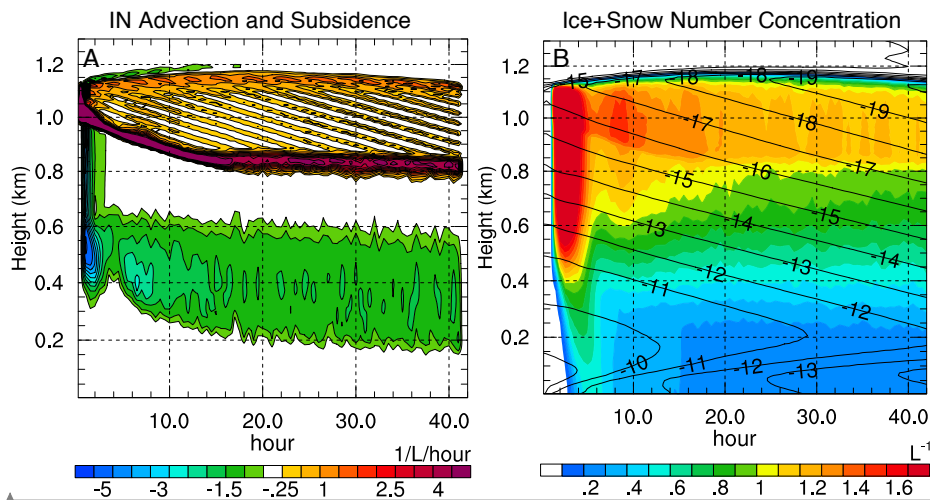
1480 concentrations. Ice water mixing ratio =  $3e-4$  g/kg, ice number concentration = 0.4/L, snow

1481 water mixing ratio =  $2.4e-2$  g/kg, snow number concentration = 0.45/L.

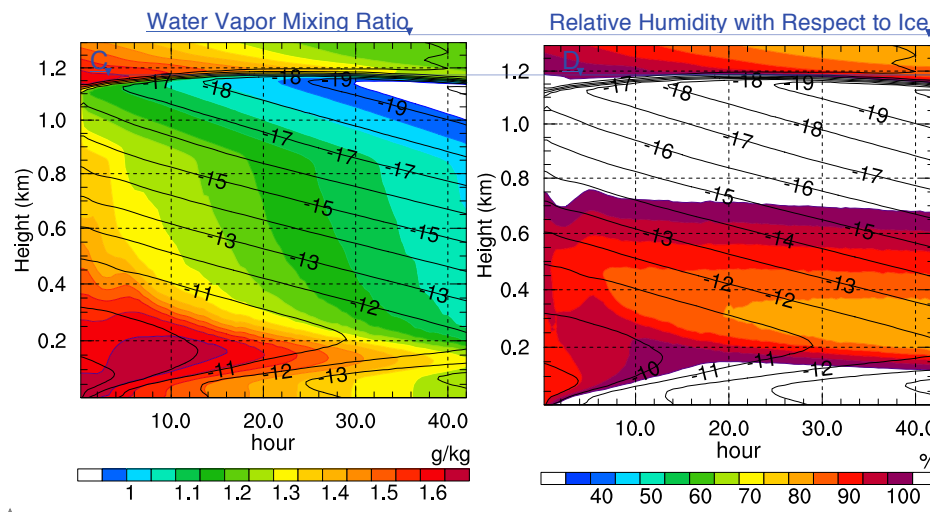
1482



1484 **Figure 6:** (A)  $N_{IN}$  and (B)  $N_{ICE}$  averaged over 0.5 hours at hour 20, in units of  $L^{-1} hr^{-1}$ . Grey  
 1485 shading indicates the extent of the cloud layer. Green dash lines indicate the top and bottom  
 1486 of the mixed layer.



1488



1489

1490 **Figure 7:** Time-height cross sections of horizontally-averaged (A) IN advection plus  
 1491 subsidence, in units of  $L^{-1}hour^{-1}$ , (B) ice plus snow number concentration, in units of  $L^{-1}$ , (C)  
 1492 water vapor mixing ratio, in units of  $g kg^{-1}$ , and (D) relative humidity with respect to ice, in  
 1493 units of percent, from CNT simulation. Temperature, in units of  $^{\circ}C$ , shown with black  
 1494 contour lines in (B,C,D).

Unknown  
 Formatted: Font:Times New Roman, 12 pt, Font color: Red

Amy Solomon 7/29/2015 10:50 PM  
 Deleted: Ice+Snow Number Concentration

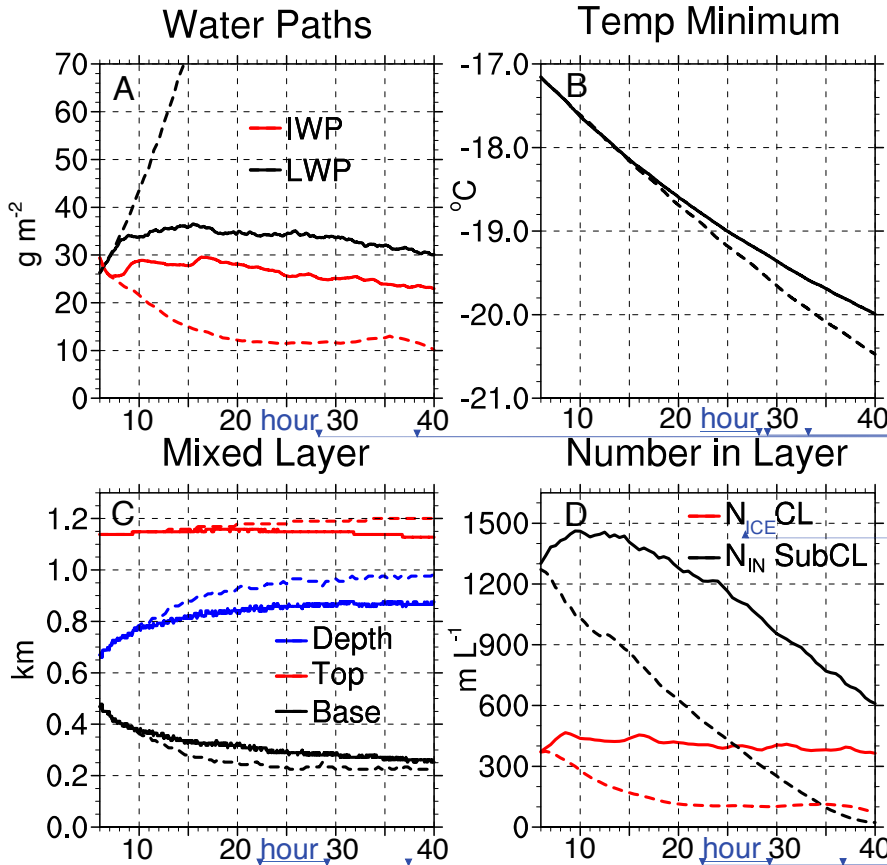
Unknown  
 Formatted: Font:Times New Roman, 12 pt, Font color: Red

Amy Solomon 7/29/2015 10:50 PM  
 Deleted: Ice+Snow Number Concentration

Amy Solomon 7/29/2015 10:45 PM  
 Deleted: A

Amy Solomon 7/29/2015 10:44 PM  
 Deleted: A

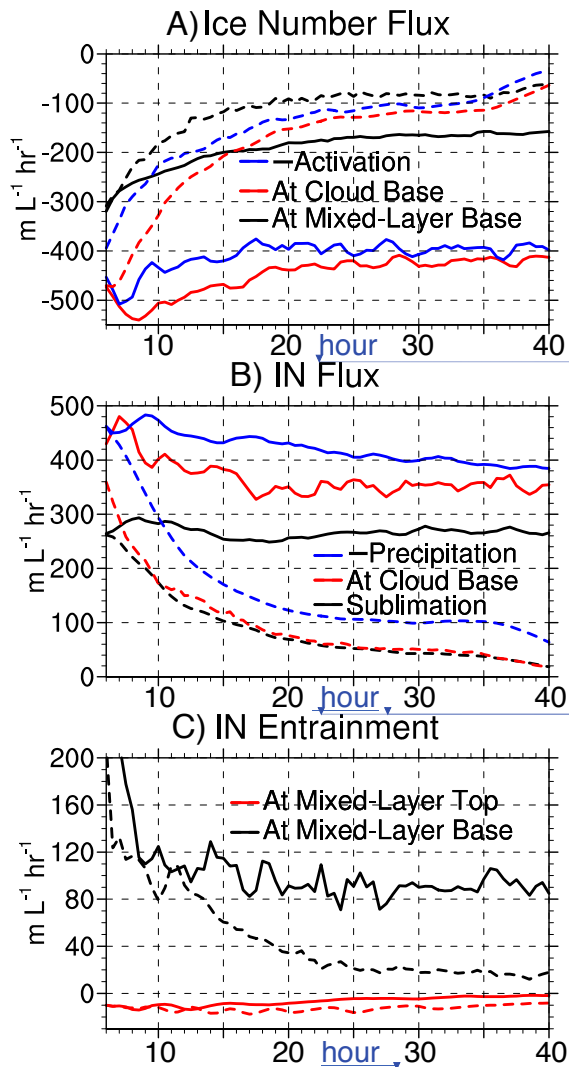
Amy Solomon 7/29/2015 3:51 PM  
 Deleted: , and (B) IN advection plus subsidence, in units of  $L^{-1}hour^{-1}$



1498

1499 **Figure 8:** Control and NoRecycle time series for hours 6-40 (smoothed with 90 minute  
 1500 running average). NoRecycle shown with red and black dashed lines. A) LWP (black) and  
 1501 IWP (red), in units of  $g\ m^{-2}$ . B) Minimum horizontally-averaged temperature in the column,  
 1502 in units of  $^{\circ}C$ . C) Mixed-layer depth (blue), top height (red), and base height (black), in units  
 1503 of km. D)  $N_{ICE}$  integrated over cloud layer (referred to as CL, red) and  $N_{IN}$  integrated over  
 1504 subcloud layer (referred to as SubCL, black), in units of  $m\ L^{-1}$  (i.e., meters/liter).

- Amy Solomon 7/29/2015 3:56 PM Deleted:
- Amy Solomon 7/29/2015 3:56 PM Deleted:
- Amy Solomon 7/29/2015 3:57 PM Deleted:
- Amy Solomon 7/29/2015 3:57 PM Deleted:
- Amy Solomon 7/29/2015 3:57 PM Deleted:
- Amy Solomon 7/29/2015 6:19 PM Formatted: Font:(Default) Arial, 9 pt
- Amy Solomon 7/29/2015 3:58 PM Deleted:
- Amy Solomon 7/29/2015 3:58 PM Deleted:
- Amy Solomon 7/29/2015 3:58 PM Deleted:
- Amy Solomon 7/29/2015 3:58 PM Deleted:
- Amy Solomon 7/29/2015 3:58 PM Deleted:
- Amy Solomon 7/29/2015 3:58 PM Deleted:
- Amy Solomon 7/28/2015 9:51 PM Deleted: 7
- Amy Solomon 7/29/2015 6:19 PM Deleted: N



Amy Solomon 7/29/2015 3:59 PM  
Deleted:

Amy Solomon 7/29/2015 3:59 PM  
Deleted:

Amy Solomon 7/29/2015 3:59 PM  
Deleted:

Amy Solomon 7/29/2015 3:59 PM  
Deleted:

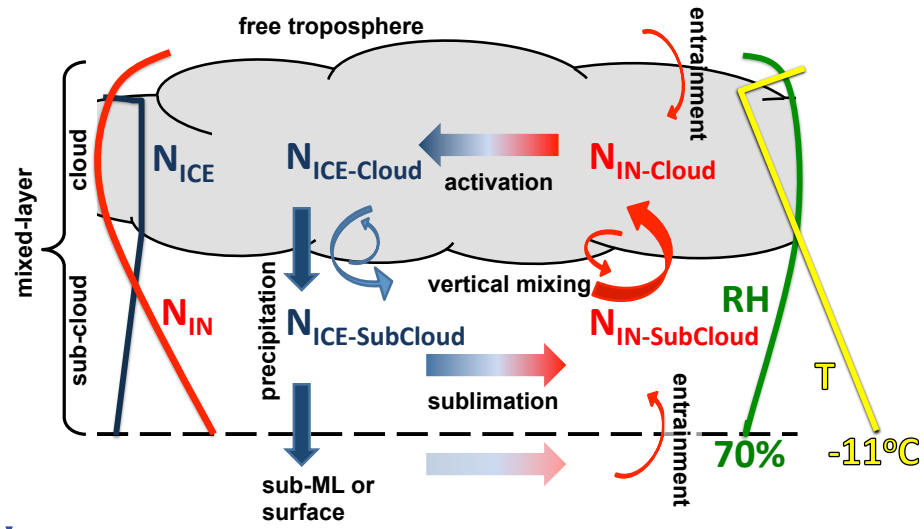
Amy Solomon 7/28/2015 9:51 PM  
Deleted: 8

Amy Solomon 7/29/2015 6:22 PM  
Deleted: N

1507

1508 **Figure 9:** Horizontally-averaged fluxes from Control and NoRecycle integrations for hours  
 1509 6-40 (smoothed with 90 minute running average). NoRecycle shown with dashed lines. A)  
 1510  $N_{IN}$  flux at cloud base due to turbulence+subsidence+precipitation (red), mixed-layer base  
 1511 due to turbulence+subsidence+precipitation (black), and due to activation (multiplied by -1,  
 1512 blue), in units of  $m L^{-1} hr^{-1}$ . B)  $N_{IN}$  flux at cloud base due to turbulence (red),  $N_{IN}$  flux due to  
 1513 sublimation (black), and precipitation of  $N_{ICE}$  at cloud base (multiplied by -1, blue), in units  
 1514 of  $m L^{-1} hr^{-1}$ . C)  $N_{IN}$  entrainment at mixed-layer top (red) and base (black), in units of  $m L^{-1}$   
 1515  $hr^{-1}$ .



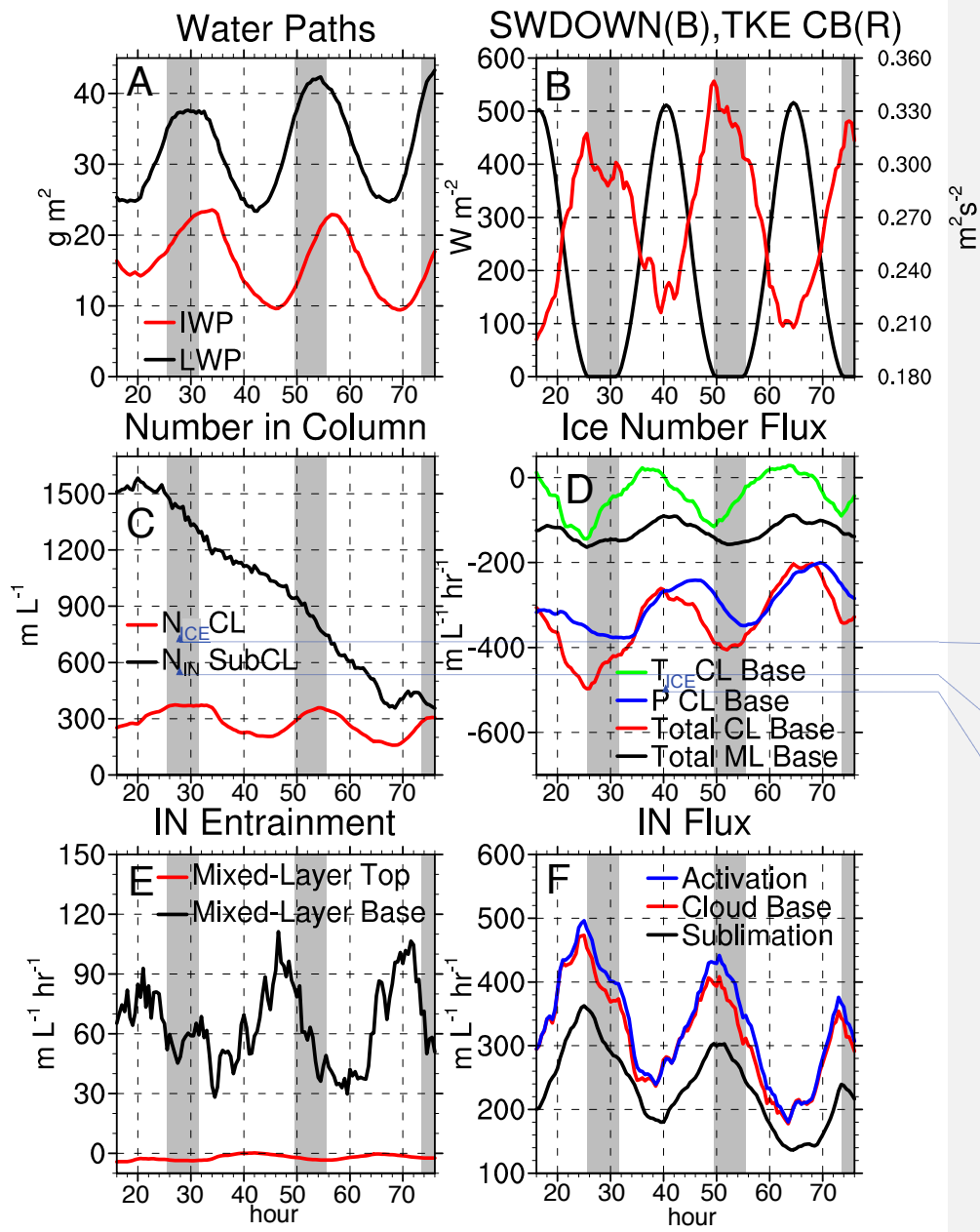


1518

1519 **Figure 10:** Schematic of feedback loops that maintain ice production and the phase-  
 1520 partitioning between cloud liquid and ice in AMPS when recycling is allowed. Red colors  
 1521 denote  $N_{IN}$ . Blue colors denote  $N_{ICE}$ . Vertical profiles of  $N_{ICE}$ ,  $N_{IN}$ , relative humidity, and  
 1522 temperature shown with thin blue, red, green, and yellow lines, respectively.

Amy Solomon 7/29/2015 6:35 PM

Deleted:  
 Amy Solomon 7/28/2015 9:51 PM  
 Deleted: 9  
 Amy Solomon 7/29/2015 6:35 PM  
 Deleted: N  
 Amy Solomon 7/29/2015 6:35 PM  
 Deleted: N



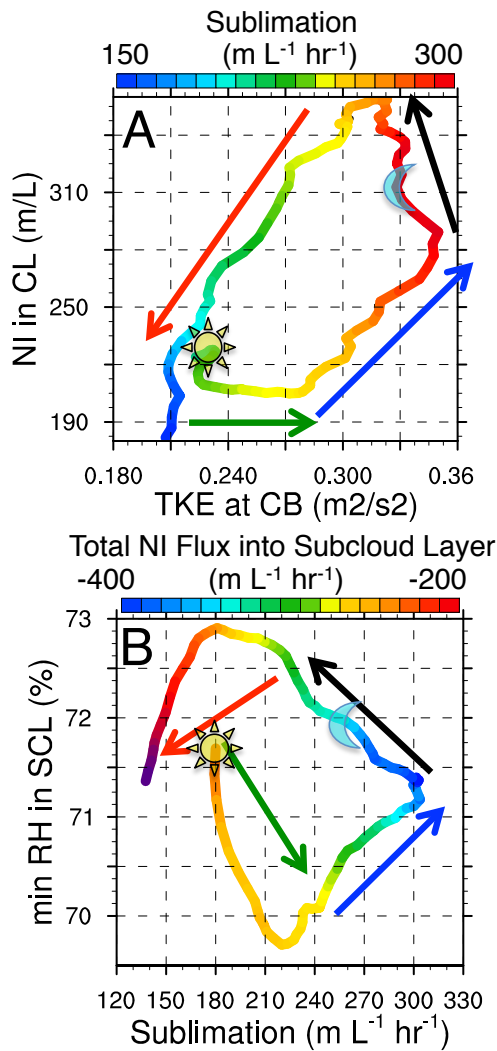
Amy Solomon 7/29/2015 6:23 PM  
 Formatted: Font:(Default) Arial, 14 pt, Subscript  
 Amy Solomon 7/29/2015 6:23 PM  
 Formatted: Font:(Default) Arial, 14 pt  
 Amy Solomon 7/29/2015 6:19 PM  
 Formatted: Font:(Default) Arial, 9 pt

1527

1528

Figure 11: SW time series (see Figure captions).

Amy Solomon 7/28/2015 9:51 PM  
 Deleted: 0



1530

1531 | **Figure 12:** A) Phase diagram of TKE at cloud base vs.  $N_{ICE}$  in the cloud layer starting at  
 1532 | peak shortwave hour 40, in units of m L<sup>-1</sup> and m L<sup>-1</sup> hr<sup>-1</sup>, respectively. Colors show  
 1533 | sublimation in units of m L<sup>-1</sup> hr<sup>-1</sup>. B) 24-hour phase diagrams of sublimation vs. minimum  
 1534 | relative humidity in the subcloud layer starting at peak shortwave hour 40, in units of m L<sup>-1</sup>  
 1535 | hr<sup>-1</sup> and %, respectively. Colors show total  $N_{ICE}$  flux at cloud base, m L<sup>-1</sup> hr<sup>-1</sup>. Hours 42-47,  
 1536 | 47-50, 50-56, and 57-62 indicated with green, blue, black, red arrows, respectively.

Amy Solomon 7/28/2015 9:51 PM

Deleted: 1

Amy Solomon 7/29/2015 6:27 PM

Deleted: NI

Amy Solomon 7/29/2015 6:27 PM

Deleted: N

1540 Minimum shortwave indicated with the moon symbol. Maximum shortwave indicated with  
1541 the sun symbol.